1231745

THE UNITED STATES OF AMERICA

TO ALL TO WHOM THESE PRESENTS SHALL COME:

UNITED STATES DEPARTMENT OF COMMERCE

United States Patent and Trademark Office

September 29, 2004

THIS IS TO CERTIFY THAT ANNEXED HERETO IS A TRUE COPY FROM THE RECORDS OF THE UNITED STATES PATENT AND TRADEMARK OFFICE OF THOSE PAPERS OF THE BELOW IDENTIFIED PATENT APPLICATION THAT MET THE REQUIREMENTS TO BE GRANTED A FILING DATE.

APPLICATION NUMBER: *60/498,742*
FILING DATE: *August 28, 2003*
RELATED PCT APPLICATION NUMBER: *PCT/US04/27893*

Certified by

Jon W Dudas

Acting Under Secretary of Commerce
for Intellectual Property
and Acting Director of the U.S.
Patent and Trademark Office

Please type a plus sign (+) inside this box → [+]

PTO/SB/16 (8-00)
Approved for use through10/31/2002. OMB 0651-0032
U.S. Patent and Trademark Office; U.S. DEPARTMENT OF COMMERCE
Under the Paperwork Reduction Act of 1995, no persons are required to respond to a collection of information unless it displays a valid OMB control number.

08/28/03 15866 U

PROVISIONAL APPLICATION FOR PATENT COVER SHEET

This is a request for filing a PROVISIONAL APPLICATION FOR PATENT under 37 CFR 1.53(c).

08/28/03 22154 U.S. PTO 60/408142

INVENTOR(S)		
Given Name (first and middle [if any])	Family Name or Surname	Residence (City and either State or Foreign Country)
Fang-Fang	Yin	Canton, Michigan
Jae Ho	Kim	West Bloomfield, Michigan
Hui	Yan	Detroit, Michigan

☐ *Additional inventors are being named on th____ separately numbered sheets attached hereto*

TITLE OF THE INVENTION (280 characters max)

FUZZY LOGIC GUIDED INVERSE TREATMENT PLANNING

Direct all correspondence to: **CORRESPONDENCE ADDRESS**

☐ Customer Number [ ] →

OR *Type Customer Number here*

Place Customer Number Bar Code Label here

☒ Firm *or* Individual Name	KOHN & ASSOCIATES, PLLC				
Address	30500 Northwestern Highway				
Address	Suite 410				
City	Farmington Hills	State	MI	ZIP	48334
Country	US	Telephone	248.539.5050	Fax	248.539.5055

ENCLOSED APPLICATION PARTS *(check all that apply)*

☒ Specification *Number of Pages* 65 ☐ CD(s), Number [ ]

☐ Drawing(s) *Number of Sheets* [ ] ☒ Other (specify) Acknowledgement Postcard

☐ Application Data Sheet. See 37 CFR 1.76

METHOD OF PAYMENT OF FILING FEES FOR THIS PROVISIONAL APPLICATION FOR PATENT *(check one)*

☒ Applicant claims small entity status. See 37 CFR 1.27.

☒ A check or money order is enclosed to cover the filing fees

☒ The Commissioner is hereby authorized to charge filing fees or credit any overpayment to Deposit Account Number 11-1449

☐ Payment by credit card. Form PTO-2038 is attached.

FILING FEE AMOUNT ($) $80.00

The invention was made by an agency of the United States Government or under a contract with an agency of the United States Government.

☒ No.

☐ Yes, the name of the U.S. Government agency and the Government contract number are: _____

Respectfully submitted,

SIGNATURE [signature]

Date 8/28/03

TYPED or PRINTED NAME Amy E. Rinaldo

REGISTRATION NO. *(if appropriate)* 45,791

Docket Number: 1059.00091

TELEPHONE 248.539.5050

USE ONLY FOR FILING A PROVISIONAL APPLICATION FOR PATENT

This collection of information is required by 37 CFR 1.51. The information is used by the public to file (and by the PTO to process) a provisional application. Confidentiality is governed by 35 U.S.C. 122 and 37 CFR 1.14. This collection is estimated to take 8 hours to complete, including gathering, preparing, and submitting the complete provisional application to the PTO. Time will vary depending upon the individual case. Any comments on the amount of time you require to complete this form and/or suggestions for reducing this burden, should be sent to the Chief Information Officer, U.S. Patent and Trademark Office, U.S. Department of Commerce, Washington, D.C. 20231. DO NOT SEND FEES OR COMPLETED FORMS TO THIS ADDRESS. SEND TO: Box Provisional Application, Assistant Commissioner for Patents, Washington, D.C.

PROVISIONAL APPLICATION COVER SHEET
Additional Page

PTO/SB/16 (8-00)
Approved for use through 10/31/2002. OMB 0651-0032
U.S. Patent and Trademark Office; U.S. DEPARTMENT OF COMMERCE
Under the Paperwork Reduction Act of 1995, no persons are required to respond to a c ollection of information unless it displays a valid OMB control number.

Docket Number	1059.00091	Type a plus sign (+) inside this box →	+

INVENTOR(S)/APPLICANT(S)

Given Name (first and middle [if any])	Family or Surname	Residence (City and either State or Foreign Country)

CERTIFICATE OF MAILING BY "EXPRESS MAIL"

"EXPRESS MAIL" Mailing Label Number EL976237205US

Date of Deposit 8/28/03

I hereby certify that this paper or fee is being deposited with the United States Postal Service "Express Mail Post Office To Addressee" service under 37 CFR 1.10 on the date indicated above and is addressed to the Assistant Commissioner for Patents, Washington, D.C. 20231.

Angel Webb

(Signature of person mailing paper or fee)

Number 2 of 2

WARNING: Information on this form may become public. Credit card information should not be included on this form. Provide credit card information and authorization on PTO-2038.

Attorney Docket No: 1059.00091
Express Mail Number: EL976237205US

PROVISIONAL PATENT APPLICATION

FUZZY LOGIC GUIDED INVERSE TREATMENT PLANNING

BACKGROUND OF THE INVENTION

TECHNICAL FIELD

The present invention relates to inverse treatment planning. More specifically, the present invention relates to an artificial intelligence method for guiding inverse treatment planning.

BACKGROUND ART

Modern day radiation therapy of tumors has two goals: eradication of the tumor and avoidance of damage to healthy tissue and organs present near the tumor. It is known that a vast majority of tumors can be eradicated completely if a sufficient radiation dose is delivered to the tumor; however, complications may result from use of the necessary effective radiation dose, due to damage to healthy tissue which surrounds the tumor, or to other healthy body organs located close to the tumor. The goal of conformal radiation therapy is to confine the delivered radiation dose to only the tumor volume defined by the outer surfaces of the tumor, while minimizing the dose of radiation applied to surrounding healthy tissue or adjacent healthy organs.

Conformal radiation therapy has been traditionally approached through a range of techniques, and typically uses a linear accelerator ("LINAC") as the source of the radiation beam used to treat the tumor. The linear accelerator typically has a radiation beam source that is rotated about the patient and directs the radiation beam toward the tumor to be treated. The beam intensity of the radiation beam is predetermined, constant beam intensity. Multileaf collimators, which have multiple leaf, or finger,

projections that can be moved individually into and out of the path of the radiation beam, can be programmed to follow the spatial contour of the tumor as seen by the radiation beam as it passes through the tumor, or the "beam's eye view" of the tumor during the rotation of the radiation beam source, which is mounted on a rotatable gantry of the linear accelerator. The multiple leaves of the multileaf collimator form an outline of the tumor shape as presented by the tumor volume in the direction of the path of travel of the radiation beam, and thus block the transmission of radiation to tissue disposed outside the tumor's spatial outline as presented to the radiation beam, dependent upon the beam's particular radial orientation with respect to the tumor volume.

Another approach to conformal radiation therapy involves the use of independently controlled collimator jaws that can scan a slit field across a stationary patient at the same time that a separate set of collimator jaws follows the target volume as the gantry of the linear accelerator rotates. An additional approach has been the use of attachments for LINACs that allow a slit to be scanned across the patient, the intensity of the radiation beam in the entire slit being modified as the slit is being scanned.

A further approach for conformal radiation therapy treatment has been the use of a narrow pencil beam of high energy photons, whose energy can be varied, and the beam is scanned over the tumor target volume so as to deliver the best possible radiation dose distribution in each orientation of the gantry upon which the photon beam source is mounted.

A major problem associated with such prior art methods of conformal radiation therapy are that if the tumor volume has concave borders, or surfaces, varying the spatial configuration, or contour, of the radiation beam, the therapy is only successful part of the time. In particular, when the convolutions, or outer surfaces, of a tumor are re-entrant, or concave, in a plane parallel to the path of the radiation treatment beam, healthy tissue or organs may be disposed within the concavities formed by the outer

tumor concave surfaces, as well as the fact that the thickness of the tumor varies along the path of the radiation beam.

In order to be able to treat tumors having concave borders, it is necessary to vary the intensity of the radiation beam across the surface of the tumor, as well as vary the outer configuration of the beam to conform to the shape of the tumor presented to the radiation beam. The beam intensity of each radiation beam segment should be able to be modulated to have a beam intensity related to the thickness of the portion of the tumor through which the radiation beam passes. For example, where the radiation beam is to pass through a thick section of a tumor, the beam intensity should be higher than when the radiation beam passes through a thin section of the tumor.

Dedicated scanning beam therapy machines have been developed wherein beam intensity modulation can be accomplished through the use of a scanning pencil beam of high energy photons. The beam intensity of this device is modulated by increasing the power of its electron gun generating the beam. The power increase is directed under computer control, as the gun is steered around the tumor by moving the gantry upon which it is mounted and the table upon which the patient lies. The effect is one of progressively "painting" the target with the thickness, or intensity, of the paint, or radiation beam intensity, being varied by the amount of paint on the brush, or how much power is applied to the electron gun, as the electron gun moves over the tumor. Such dedicated scanning beam therapy machines, which utilize direct beam energy modulation, are expensive and quite time consuming in their use and operation, and are believed to have associated with them a significant patient liability due to concerns over the computer control of the treatment beam itself.

Other methods and apparatus for conformal radiation therapy have been developed that spatially modulate the beam intensity of a radiation beam across a volume of tissue in accordance with the thickness of the tumor in the volume of tissue by utilizing a plurality of radiation beam segments. Such methods and apparatus utilize attenuating leaves, or shutters, in a rack positioned within the radiation beam before the

beam enters the patient. The tumor is exposed to radiation in slices, each slice being selectively segmented by the shutters. However, a minor disadvantage of that method and apparatus results from the fact that only two slices of tissue volume may be treated with one rotation of the gantry of the linear accelerator. Although the slices may be of arbitrary thickness, greater resolution is accomplished by selecting slices for treatment that are as thin as possible. As the thickness of the treatment slices decreases, the time it takes to treat the patient increases because more treatment slices are required in order to treat the entire tumor volume.

The foregoing methods and apparatus are designed to minimize the portion of the structures being exposed to radiation. However, because exposure to surrounding structures cannot be completely prevented, treatment plans are desired that are optimized to eradicate the tumor volume while minimizing the amounts of radiation delivered to the surrounding structures. Existing methods and apparatus for optimizing treatment plans use a computer to rate possible plans based on score functions which simulate a physician's assessment of a treatment plan. However, existing methods and apparatus have proven to be insufficient.

Existing methods and apparatus utilize a computational method of establishing optimized treatment plans based on an objective cost function that attributes costs of radiation of various portions of both the tumor and surrounding tissues, or structures. One such computational method is known in the art as simulated annealing. Existing simulated annealing methods utilize cost functions that consider the costs of under-exposure of tumor volumes relative to over-exposure of surrounding structures. However, the cost functions used in existing methods do not account for the structure volumes as a whole, relying merely on costs related to discrete points within the structure, and further do not account for the relative importance of varying surrounding structure types. For example, certain structure types are redundant in their function and substantial portions of the structure volume can be completely eradicated while retaining their function. Other structure types lose their function if any of the structure is completely eradicated. Therefore, the more sensitive structure volumes can receive a

measured dose of radiation so long as no portion of the structure is subjected to a lethal dose.

Existing cost functions utilized in the optimization of treatment plans do not account for such varying costs associated with the different types of structures. After the treatment plan is optimized, the physician currently must evaluate each computed treatment plan for compliance with the desired treatment objective. If the computed treatment plan does not successfully meet the treatment objectives, the optimization process is repeated until a treatment plan can be computed that meets the physician's treatment objectives for both the tumor volume and the surrounding structures. Further, existing methods and apparatus do not allow the physician to utilize the familiar Cumulative Dose Volume Histogram ("CDVH") curves in establishing the desired dose distributions.

Prior to the development of the present invention, there has been no method or apparatus for conformal radiation therapy, for use with a radiation beam having a predetermined, constant beam intensity for treatment of a tumor which: is simple and economical to use; that has what is believed to be a high safety factor for patient safety; computes an optimal treatment plan to meet conflicting, pre-determined, treatment objectives of a physician, accounting for objectives in both the target tumor volume and multiple structure types; and utilizes provides the desired dose distributions for each target tumor volume and tissue and structure types.

DESCRIPTION OF THE INVENTION

An artificial intelligence (AI) method, fuzzy logic, is applied to optimize parameters in the inverse treatment planning for intensity-modulated radiation therapy (IMRT). With the capability of fuzzy inference, the parameter modification of the objective function is guided by physician's treatment intention and experience. For the different parameters involving inverse planning, the corresponding fuzzy inference systems (FISs) are developed in order to accomplish the treatment requirement. With the use of fuzzy inference, the efficiency and quality of inverse planning can be

substantially improved.

The present invention provides a method of using fuzzy logic to optimize treatments of patients. More specifically, the present invention uses a fuzzy inference systems that uses three modules: a Fuzzifier, a Inference engine, that includes fuzzy rules, and a Defuzzifier. During the process of fuzzification a single input value is compared to the membership functions as defined for that input variable. If the membership functions have a nonzero output it will take effect in the final results of the FIS. The Fuzzifier calculates the response of rules for the input values and the inference engine modifies the consequent rules in response to input values. The Defuzzifier generates a final output based on the result of the inference engine.

Preferably, a computer is utilized to automatically calculate this in response to the input of data, however, a human can also calculate the same using the formula show in Appendix A. A detailed description of formula is set forth in Appendix A included herewith and incorporated by reference in its entirety.

APPENDIX A

IP application for
artificial intelligence guided inverse planning system

Title: Artificial Intelligence-guided Inverse Treatment Planning

Abstract: An artificial intelligence (AI) method, fuzzy logic, is applied to optimize parameters in the inverse treatment planning for intensity-modulated radiation therapy (IMRT). With the capability of fuzzy inference, the parameter modification of the objective function is guided by physician's treatment intention and experience. For the different parameters involving inverse planning, the corresponding fuzzy inference systems (FISs) are developed in order to accomplish the treatment requirement. With the function of fuzzy inference, the efficiency and quality of inverse planning will be substantially improved.

Introduction:

The conventional inverse treatment planning involves optimizing an intensity spectrum by an objective function in order to obtain an ideal dose distribution. Sometimes, the dose distribution calculated by the optimized intensity spectrum might not be the one we expected. It is often resulted by an improper selection of parameters selected in the objective function. As the desired dose distribution can only be achieved by a refined combination of parameters that are usually unknown, it was inevitable for a planner to try different combinations of parameters in order to achieve a desired dose distribution. At present, this process is done by a trial-and-error approach.[1-10] It is not only time-consuming but also difficult to find a desired combination of parameters.

A number of methods have been proposed in recent years in order to tackle this problem.[4,7,12-16] Starkschall[12] proposed an approach that removed the necessity of defining a "best" treatment plan, and incorporated the dose-volume constraints into a system to search for a feasible plan that could satisfy the constraints. If no calculated doses satisfy the treatment goal, the planner will provide a guide about how the dose-volume constraints may be modified to achieve a feasible result. This approach is only applied to the conventional three-dimensional (3D) treatment planning. Wu and Mohan[4] developed an optimization system, which employed both dose- and dose-volume-based objective functions. In their system, the optimal plan is selected by calculating the cost of the objective function, or "plan score" (the lower the score, the better the plan). Xing et al.[13,14] presented a method which employed a second stage evaluation function to compute the differences between the calculated and the ideal dose volume histograms. Based on the results of the evaluation function, the weighting factors in the objective function are adjusted. This procedure is to minimize both the objective and evaluation functions in a round-robin manner. Later, further improvement is achieved by using a statistical measure called preference function, which is constructed based on the empirical judgment. The problem about the selection of weighting factor still exists because it translated to the problem of how to specify the parameters in the evaluation or preference function. A similar method was also proposed by Wu et al.[15] using a genetic algorithm to optimize the weighting factors and beam weights in the conventional 3D

treatment planning. Li and Yin[7] introduced fuzzy logic into the inverse planning system to adjust the weighting factors for normal tissue. The result was promising. However, optimizing the parameters for the target and critical organ were not included in the system. Also, the weighting factors initialized by the fuzzy functions still need to be modified by the trial-and-error approach.

Purpose:

One of the major advantages of IMRT is to spare dose of the critical organ adjacent to the target. When a strict compromise between target dose and critical dose was required, fine-tuning of parameters in the objective function is important and necessary. As the effect of parameters on the output of the inverse planning is uncertain, it is hard to say which combination of parameters is best for the current case. Generally, this decision is made according the priority of organs involved and is individualized. More concerns will pay to the organ with high priority. As the trial-and-error approach can be regarded as a way using empirical knowledge to guide the parameter modification, it can be substitute by existed AI approaches, such as expert system and fuzzy inference system.

The main purpose of this research is to use fuzzy interference system to define parameters in the objective function based on treatment intention instead of trial-and-error approach.

Detailed description

See attached manuscripts.

The advantage provided by the invention

Will improve the accuracy and efficiency of inverse treatment planning for IMRT. Specifically,

(1) The heuristic and practical experience (from physician, physicist, planner) can be used to guide the optimizing the parameters of inverse planning in order to improve the dose distribution;
(2) The conformity of target dose distribution can be improved and high target dose could be feasible – improve the quality of inverse planning;
(3) The time spent on trial-and-error test can be reduced significantly and the planner will be free from this time-consuming task – improve the efficiency of inverse planning.

Commercial significance of that advantage:

It will make the treatment planning system more competitive.

The closest known prior publications and prior uses, if any.

1. J. Liacer, "Inverse radiation treatment planning using the dynamically penalized likelihood method," Med. Phys. 24,1751-1764 (1997).
2. H. Dimitre and B. Gino, "A continuous penalty function method for inverse treatment planning," Med. Phys. 25,208-223 (1998).
3. P. S. Cho and S. Lee, "Optimization of intensity modulated beams with volume constraints using two methods: Cost function minimization and projections onto convex sets," Med. Phys. 25, 435-443 (1998).
4. Q. Wu and R. Mohan, "Algorithms and functionality of an intensity modulated radiotherapy optimization system," Med. Phys. 27, 701-711 (2000).
5. S. V. Spirou and C.S. Chui, "A gradient inverse planning algorithm with dose-volume constraints," Med. Phys. 25, 321-333 (1998).
6. I. Rosen, R. G. Lane, "Treatment plan optimization using linear programming," Med. Phys. 18, 141-152 (1991).
7. R. P. Li and F. F. Yin, "Optimization of inverse treatment planning using a fuzzy weight function," Med. Phys. 27, 691-700 (2000).
8. H. Yan, F. F. Yin, H. Q. Guan, and J. H. Kim, "The Fuzzy Logic Guided Inverse Treatment Planning," submitted by Med.Phys. 2002.
9. S. Webb, "Optimization of conformal radiotherapy dose distributions by simulated annealing," Phys. Med. Biol. 34, 1349-1370(1989).
10. Y. Liu, F. F. Yin and Q. Gao, "Variation method for inverse treatment," Med. Phys. 26, 356-363 (1999).
11. S. Webb, Intensity-modulated radiation therapy, (Institute of Physics Publishing, Bristol, UK, 2001).
12. G. Starkschall and A. Pollack, "Treatment planning using a dose-volume feasibility search algorithm," Int. J. Rad. Onc. Bio. Phys. 49, 1419-27(2001).
13. L. Xing and J. Li, "Optimization of importance factors in inverse planning," Phys. Med. Biol. 44, 2525-2536 (1999).
14. L. Xing and J. Li, "Estimation theory and model parameter selection for therapeutic treatment plan optimization," Med. Phys. 26, 2348-2358 (1999).
15. X. G. Wu and Y. P. Zhu, "An optimization method for importance factors and beam weights based on genetic algorithms for radiotherapy treatment planning," Phys. Med. Biol. 46,1085-1099, (2001).

SECTION 2 – RESEARCH PLAN

A. SPECIFIC AIMS:

The objective of this proposal is to develop an optimal approach for inverse treatment planning and a three-dimensional verification method for intensity-modulated radiation therapy. Specifically, this study will test two hypotheses:

(1) The vague prescription could be represented by the theory of fuzzy set in inverse treatment planning.
(2) The dose distribution delivered by limited number of static intensity-modulated radiation fields can be directly verified using a three-dimensional reconstruction method.

The specific approaches to test these hypotheses are to:

(1) Develop an effective inverse planning method to test prescription method and generate intensity spectrum for intensity-modulated radiation therapy.
(2) Develop a logical fuzzy function to represent the vague dose prescription in the inverse-planning algorithm.
(3) Develop a three-dimensional CT reconstruction algorithm for patient anatomy using a limited number of projections.
(4) Develop a method to reconstruct dose distribution in 3-D CT images based on a limited number of static IMRT fields using multilevel algebraic reconstruction technique.

B. SIGNIFICANCE:

It has been shown that the tumor loco-regional control can be improved with higher radiation dose than conventional prescription (Ref.?). However, delivery of higher dose is typically associated with the increase of probability of normal tissue complications. One approach to reduce this complication is to minimize the volume of normal tissue irradiated (ref.?). To achieve this goal, it will need a conformal dose distribution to target volume, a dedicated dose delivery mechanism, and a verification method for patient positioning and dose delivered.

Recent studies indicated that conformal dose distribution could be effectively achieved with the treatment technique called intensity-modulated radiation therapy (IMRT) (Ref.?). Several promising delivery devices have also become available, such as static or dynamic MLC and tomotherapy to deliver conformal radiation dose (Ref. ?). The basic concept of IMRT is that a dedicated delivery device with an intensity-variable modulates a uniform intensity in a traditional treatment field. However, it is still a very challenging issue in terms of how to generate an effective and optimal intensity spectrum and how to verify modulated radiation delivery. The first issue is also related to the problem of inverse treatment planning (or treatment planning optimization).

Inverse planning method describes a specific treatment planning procedure in which, differing from traditional approach, both dose and volume are given first. Then a set of modulated beams is generated through a computer-aided optimization process in order to satisfy the

prescription. This process is extremely important if the shapes of the target and critical organs are complicated, especially when the target has concavity and a critical organ lies in the hollow of the concavity. Typically, inverse treatment planning for intensity modulated radiation therapy involves the selection of an objective function and method of optimization. For a given objective function, an optimal treatment plan usually requires the optimization of beam intensity elements, a prescription method, and beam number and orientation.

One of the most challenging problems in the optimization of treatment planning is how to construct a model by which the aim of radiation therapy can be fulfilled. The models that have been studied in the past can be classified as either physical or biological. There have been detailed discussions in recent literature (Ref. 1,11) concerning the merits and limitations of these two types of models. While biological models may be able to directly measure the clinical outcome, they still remain in the formative stages and suffer from controversy concerning the validity of the radiobiological response data used (such as, tumor control probability (TCP) and normal tissue complication probability (NTCP)) (Ref. 1, 13-15). On the other hand, the physical dosimetric prescription has been well established as the clinical norm. In the traditional physical models, one optimizes an objective function that is the measure of closeness of the calculated dose distribution to the prescribed dose distribution. The crucial problem here is how to give the optimal dose value for the normal tissue so that the two objectives, delivering the desired dose to the target volume and minimizing the dose to normal tissues, can be achieved accordingly.

A quadratic model has typically being used in inverse treatment planning. The model is widely discussed and has two major limitations, no direct biological information and no minimal constraints to normal tissues. Linguistically, the purpose of radiotherapy may be stated as (a) delivering a desired tumor dose and zero dose outside the target volume; (b) delivering a high dose to the target volume and a low dose to the normal tissue. The statement (a) and (b) may be served as absolute linguistic prescription (ALP) and relative linguistic prescription (RLP), respectively. Although the ALP is ideal, it is clearly impossible to deliver due to the laws of nature [2]. On the other hand, RLP clinically describes the strategy of radiation therapy. The words 'high' and 'low' used here are vague terms that are associated with the limitation of making precise definition. The complexity of treatment planning optimization is evident from the need to formulate some kinds of clinical goals to be optimized since there is no unique treatment plan which is clinically feasible and fulfills the two conflicting objectives: maximizing dose in the target volume while minimizing dose in normal tissues.

Recently, several researchers [6]-[8] have come to pay attention to the analysis of uncertainties in radiation treatment planning optimization. The tolerance of normal tissues has been discussed in [6] and [12]. Spirou et al [16] developed an inverse planning algorithm with soft constraints. The method allows acceptable doses of maximum and minimum as well as dose-volume constraints to the tissues of interest.

The search for the optimal beams can usually be interpreted to be an optimization problem. Thus, the searching problem is converted to find the extremum of a given objective function. Several methods and algorithms have been investigated for inverse planning. Some examples are simulated annealing,[1-4] iterative approaches,[5-10] as well as filtered back-projection and Fourier transformation.[6,7,11-14] Although these methods are very promising, there are some aspects that can

be further improved upon. The simulated annealing method may require long computation time due to the nature of random search. Most iterative approaches are parameter-dependent. The convergence and the quality of convergence may be affected by these parameters which are often determined by try-and-error. The filtered back-projection and direct Fourier transformation may have limitations on dose prescription and kernel selection. Inverse treatment planning is still at its early stage and many important aspects require be to further improved.

In this research proposal, a new inverse planning method is introduced. A fuzzy approach is proposed to optimize the prescription of normal tissue. The presented method is based on the theory of fuzzy sets [9], and attempts to sufficiently use uncertain information under the tolerance. This new method contains two types of optimizations: intensity-modulated beam optimization and normal tissue prescription optimization. The former employs the fast-monotonic descent (FMD) technique. In this technique, a new iteration method is being developed in which the update scheme is analytically determined to avoid defected convergence.

Execution of IMRT conformal plan using a dedicated delivery system requires accurate patient positioning. If patient is no correctly positioned, conformal radiation beams may be delivered to normal tissues rather than the planned target. Therefore, patient mis-positioning may limit the applicability of dose escalation that is the key for IMRT.

A conventional radiation field is documented by use of a portal film in two-dimensional version. Information included in this image may not sufficient for IMRT procedure, because the leaf position is not stationary during treatment for each field. Most quality assurance procedures for IMRT are performed in phantom. It is therefore, important to find a way to verify both anatomically and dosimetrically for IMRT treatment. It has been noted that monitoring actual dose delivered in IMRT using megavoltage computed tomography (MVCT) and portal imaging taken together with transit dosimetric method grows in great importance [Webb]. At present, a rapid and cost-effective method of verifying conformal IMRT radiotherapy based on limited number of fields is currently unavailable in clinical practice.

In this proposal, a combined method will be developed to perform three-dimensional verification of patient setup and to document dose distribution treated using limited number of static IMRT fields. In this method, a megavoltage CT reconstruction technique will be developed based on Multilevel Scheme Algebraic Reconstruction Technique (MLS-ART) (Ref. ?) using a megavoltage x-ray imaging device. By combining the transmitted treatment beams with the regular CT imaging projection beams, both patient geometry at treatment position and actual dose distribution can be reconstructed. The geometry and dose can be compared to the patient setup position and prescribed dose and used to correct subsequent beam placement or dose delivery accordingly.

Portal CT and portal dose reconstruction is a novel verification technique in radiation therapy (especially in IMRT) with several advantages. It is online and allows direct verification of IMRT for both patient position and dose delivery. Moreover, mega-voltage CT-based technology may potentially replace conventional patient simulation which uses kilo-voltage simulator or diagnostic x-ray CT and mega-voltage CT-based images may potentially be used for treatment planning.

C. PRELIMINARY STUDIES:

C.1. Fast-convergence optimization algorithm

The optimization of intensity-modulated beams (IMBs) consists of two main tasks: modeling (selection of objective function) and optimization (method of minimizing objective function). In this context, modeling means that the construction of a model in which our knowledge (physical, biological and clinical) about the irradiated structure's response to radiation is expressed by an objective function. The task of optimization is to develop a method by which one can obtain the optimal solution of minimizing the objective function.

For multilateral optimization of radiation treatment planning, how to improve computation efficiency is an important topic [13], [17] and [18]. We are developing a general iterative method for intensity-modulated beam optimization. In this method, an optimal step-length, the key parameter in the update scheme for iteration, and an optimal solution to the problem of negative intensity are analytically derived. Therefore, the convergence to global minimum is not only guaranteed but also fast and monotonic descent. This method is called fast-monotonic descent (FMD) method, that can provide an optimal solution to the intensity-modulated beams either when the intensity value is greater than zero or when a negative solution is encountered.

Let $\mathbf{x} = (x_1, x_2, ..., x_N)$ be an intensity vector; x_n is the nth component of intensity vector $\mathbf{x}$. For each dose point (i, j, k), let P_{ijk} represent the prescribed dose, and D_{ijk} denote the calculated dose

$$D_{ijk} = \sum_{n=1}^{N} A_{n,ijk} x_n , \qquad (1)$$

where $A_{n,ijk}$ is a non-negative constant coefficient that can be directly calculated. The weight $w_{ijk} \geq 0$ is used to indicate the importance of matching prescription and calculation. A quadratic objective function is therefore defined by

$$f(\mathbf{x}) = \sum_i \sum_j \sum_k w_{ijk} (P_{ijk} - D_{ijk})^2 . \qquad (2)$$

In the case of an optimization problem having an objective function of Eq.(2), the minimum cost problem is that of finding an admissible intensity vector such that objective function f is minimized. This constrained optimization problem can be written as

$$\underset{\{\mathbf{x}\}}{minimize}\{f(\mathbf{x})\} \qquad (3a)$$

$$subject\ to\ x_n \geq 0 \quad \forall n . \qquad (3b)$$

Now consider an unsynchronous updating scheme used in iteration method. For an arbitrary evolution time l, when $l \to l+1$,

$$x_n(l+1) = \begin{cases} x_n(l) + \Delta x_n & \text{if} \quad n = m \\ x_n(l) & \text{otherwise} \end{cases} \tag{4}$$

and

$$f(\mathbf{x}(l)) \to f(\mathbf{x}(l+1)),$$

where m is one of (1, 2,...,n,...,N). The updating scheme (4) says that, for each evolution time l, only one variable is adjusted. If each of variables is adjusted one time, then it is called one cycle.

Based on the theory of classical minimum, the necessary and sufficient condition of descent for f is that the iterative rule satisfies: for each n

$$\Delta x_n = -\lambda_n \frac{\partial f(\mathbf{x}(l))}{\partial x_n}, \tag{5}$$

where λ_n is a small positive number and called step-length. Note that the iteration sequence generated by Eqns (4) and (5) is not guaranteed to converge to the minimum of f. This convergence is always dependent upon the choice of λ_n. Adequate selection of this parameter is critical for the success of iteration method. Generally, the choice of λ_n is a craft that is problem-specific. We found, for a quadratic function, this parameter can be analytically derived and f will converge rapidly and monotonically to the minimum with the following condition:

$$\frac{\partial f(\mathbf{x}(l+1))}{\partial x_n} = 0 \quad \forall n. \tag{6}$$

Parameter λ_n can then be derived from the condition listed above.

$$\lambda_m = \frac{1}{2\sum_i \sum_j \sum_k w_{ijk} A_{m,ijk}^{\ 2}}. \tag{11}$$

With these two conditions (Eqns (5) and (6)), f descends rapidly to the global minimum if for each m $(1 \le m \le N)$

$$x_m(l+1)=\begin{cases} x_m(l)+\sum_{n=1}^{N} B_{mn}x_n(l)+C_m & \text{if} \quad x_m(l+1)\geq 0, \\ 0 & \text{otherwise;} \end{cases} \tag{7}$$

where l denotes the l-th iteration,

$$B_{mn}=-\frac{\sum_i\sum_j\sum_k w_{ijk}A_{m,ijk}A_{n,ijk}}{\sum_i\sum_j\sum_k w_{ijk}A_{m,ijk}^{\ 2}},$$

and

$$C_m=\frac{\sum_i\sum_j\sum_k w_{ijk}A_{m,ijk}P_{ijk}}{\sum_i\sum_j\sum_k w_{ijk}A_{m,ijk}^{\ 2}}.$$

The FMD algorithm can be summarized as follows:

1) Fix the maximum number of iterations L, weights $\{w_{ijk}\}$, and termination criterion $\varepsilon>0$.
2) Initialize $\mathbf{x}(0)=(x_1(0),x_2(0),...,x_N(0))$, and $x_n\geq 0$ for each n.
3) For l=1, 2,..., L;
   a. Update intensity vector using Eq.(4).
   b. Compute $E_l=\max_{\{n\}}\|\mathbf{x}_n(l+1)-\mathbf{x}_n(l)\|$.
   c. IF $E_l\leq\varepsilon$ stop; ELSE next l.
4) Compute dose distribution using Eq.(1).

Note that f is a constrained quadratic objective function. A set of values $x_1,x_2,...,x_N$ that satisfies the non-negative constraints expressed by Eqn (3b) is called an admissible vector, and the admissible vector that minimizes the objective function is called the optimal admissible vector. An optimal admissible vector may fail to exist for two reasons. There are no admissible vectors (i.e., the given constrains are incompatible) or there is no minimum (i.e., there exists a direction in N space where one or more of the variables can be taken to negative infinity while still satisfying the constraints). Fortunately, neither of them is satisfied in the problem of intensity-modulated beam optimization. First, it is clear that, the sets in Eqn (3b) are convex, and the intersection consists of many points. Therefore, the non-negative constraints in Eqn (3b) are compatible. The second reason is also false since the intensity variables are non-negative.

C.2. Fuzzy function for vague prescription

There is one important parameter $\{w_{ijk}\}$ in Eq.(2) that has not been addressed in the previous section. Typically, we know the prescribed dose for the target volume and the upper limit for the sensitive organ. The prescription for the normal tissue is usually not given. Therefore, the optimization result varies with the prescription selected for the normal tissue. An intuitive strategy for finding the optimal normal tissue prescription would be to compare values of objective function calculated by using different prescribed doses and then to choose the minimum. In this way, w_n, the weight for the normal tissue, is a function of p_n, the prescribed dose for the normal tissue. Here, the subscript n represents a point (i, j, k) inside the normal tissue. The difficulty of using this strategy is how to formulate the relationship between weight w_n and prescribed dose p_n. Generally, all one knows is a plausible relationship between them: w_n is the least when p_n approaches to zero and w_n is the greatest when p_n approaches to the upper limit. In this paper a dynamic weight function is used to express this fuzzy relationship. An optimal prescription dose for normal tissue is then determined by a validity function.

C.2.1 Dynamic weighting

Consider a quadratic objective function as shown in Eq. 2 with fuzzy weight as follows

$$P_{ijk} = \begin{cases} p_t, & if \quad i,j,k \in \Omega_t \\ p_s, & if \quad i,j,k \in \Omega_s \\ p_n; & if \quad i,j,k \in \Omega_n \end{cases}$$

and

$$w_{ijk} = \begin{cases} w_t, & if \quad i,j,k \in \Omega_t \\ w_s, & if \quad i,j,k \in \Omega_s \\ w_n. & if \quad i,j,k \in \Omega_n \end{cases}$$

p_t, p_s and p_n denote the prescribed doses for the target volume, the sensitive organ and the normal tissue, respectively. Ω_t, Ω_s and Ω_n represent regions of these three corresponding structures. $w_{ijk} \in [0,1]$ is called fuzzy weight function that is used to emphasize the importance of matching the prescribed dose and the calculated dose for the point (i, j, k). Instead of fixing $\{P_{ijk}\}$ and $\{w_{ijk}\}$ in the hard inverse planning (HIP), p_n is defined as a variable and w_n is represented by a function of p_n in fuzzy inverse planning (FIP). Also, it is assumed that

$$p_t = P_t,\ p_s = P_s,\ w_t = w_s = 1$$

and

$$w_n = \begin{cases} 1, & if \quad p_n > P_n \\ g(p_n), & otherwise \end{cases} \qquad (9)$$

where P_t represents the prescribed dose in the target volume, P_s is the tolerance dose in the sensitive organ, and P_n is the tolerance dose in the normal tissue. $g(p_n)$ is a continuous function that increases with p_n. $g(p_n)=1$ when p_n is equal to the tolerance dose P_n. Here $g(p_n)$ is called fuzzy weight function.

Regarding the function $g(\cdot)$, one has only some vague knowledge that can be stated by the following two fuzzy rules: 1) the closer p_n is to P_n, the closer w_n is to one (w_n =1 means the most important); 2) the closer p_n is to zero, the closer w_n is to zero (w_n =0 means the least important). Our purpose here is to use fuzzy technology to express this vague knowledge and to achieve an optimal solution. The form of fuzzy weight function may be obtained from planner's experience. As will be seen below, however, it is effective to use the following function:

$$g(p_n)=(\frac{p_n}{P_n})^K, \qquad 0\le p_n\le P_n \tag{10}$$

where K is a positive constant that controls the pattern of $g(\cdot)$. These functions are shown in Fig.1. Obviously, any function with a K value of equal to or greater than 1 can be selected to express the mathematical meaning of the following linguistic prescription. For the normal tissue, the closer the prescribed dose p_n is to the tolerance dose, the greater the importance of the lose (i.e., the difference between the tolerance dose and the prescribed dose) is.

C.2.2. Validity for inverse treatment planning

Fuzzy inverse planning allows many feasible solutions to occur for a specific clinic problem. Selection of a specific treatment plan is determined by evaluating planning validity. Note that Eq. (8) cannot be served as a validity function since the objective of radiation therapy optimization for non-target volume cannot be expressed by a quadratic function. To measure the validity of radiation treatment, we introduce a validity function, say $v(\{P_{ijk}\};\mathbf{x})$, which is written as

$$v(\{P_{ijk}\};\mathbf{x})=\sum_{i,j,k\in\Omega_t}\left|P_{ijk}-D_{ijk}\right|+\sum_{i,j,k\notin\Omega_t}D_{ijk}. \tag{11}$$

Where, the first term represents the degree of dose uniformity for the target volume, and the second term represents the grade of protection of the non-target volume. For prescription validity, we thus presume that the ideal dose distribution can be achieved by minimizing $v(\{P_{ijk}\};\mathbf{x})$ under the tolerance of normal tissues:

$$minimize\left\{v(\{P_{ijk}\};\mathbf{x})\right\}. \tag{12}$$

With the introduction of this validity function, the fuzzy inverse planning (FIP) algorithm can be summarized as follows.

The FIP Algorithm:

FIP1. Fix the maximum number of trial dose prescriptions T for normal tissue, the maximum number of iterations L, and the termination criterion $\varepsilon>0$. Choose fuzzy weight function $g(\cdot)$.

FIP2. Initialize $\mathbf{x}(0)=\left(x_1(0),x_2(0),...,x_N(0)\right)$, and $x_n \geq 0$ for each n.

FIP3. For t=1, 2,..., T

1) Given p_n (usually p_n increases with t on the interval $(0,P_n]$).
2) Calculate w_n using Eq.(9).
3) For l=1, 2,..., L
   a. Update intensity vector using Eq.(7).
   b. Compute $E_l=\max_{\{n\}}\left\|\mathbf{x}_n(l+1)-\mathbf{x}_n(l)\right\|$.
   c. IF $E_l \leq \varepsilon$ go to 4); ELSE next l.
4) Calculate v using Eq.(11).
5) IF $v_{t+1}>v_t$ stop; ELSE next t.
6) Compute dose distribution using Eq.(1).

C.3. Evaluation of fuzzy inverse planning method using phantom cases

The FIP is evaluated by two artificial examples. Dose-volume histograms (DVH) of the target volume (TV) and the sensitive organs (SO) are used as a primary tool for presenting and comparing dose distributions.

C.3.1. Case 1

This is a simulated cylindroid object and its central slice is illustrated in Fig.2. The geometry of this slice is similar to a CT head axial cut with two sensitive organs (analog to eyes) which are very close to the target volume. The prescription was given as follows: 100 dose units to the target volume, 20 dose units to the sensitive organs, and upper limit of 60 dose units to the normal tissue. Seven fan beams as shown in Fig.2 were uniformly arranged between 0-2π. Based on the primary-only model [10], the dose at depth is estimated by means of the percent depth dose data that were measured from a field size of 4x4cm with 6MV photon beams. However, beam divergence was included.

In order to show the convergence and fastness of FMD method, the FMD algorithm was run using three different values of the step-length: λ_n=0.01, $\lambda_n=\lambda_{opt}$ and λ_n=0.001 (n=1,2,...,N). Here λ_{opt} is the optimal step-length. Figure 3 shows the differences of convergence behavior between $\lambda_n=\lambda_{opt}$ and λ_n=0.001, and between $\lambda_n=\lambda_{opt}$ and λ_n=0.01 (n=1,2,...,N). This result indicates that the effectiveness of iteration methods is dependent upon the choice of step-length. The optimal step-length λ_{opt} derived here, however, provides an optimal performance in both the speed of convergence and the quality of convergence. Figure 4 shows that FMD can provide a satisfactory result after 10 cycles.

C.3.1.1. Effect of normal tissue dose

In this study, a validity function is introduced to judge the optimal normal tissue prescription. Variation of validity function v versus prescribed normal tissue dose is plotted in Fig.5. The data in Fig.5 indicated that p_n=25 dose units appears to be the optimal prescription for normal tissue. Table 1 shows the fuzzy inverse planning (FIP) performance as a function of the normal tissue prescription dose with K=5 and L=100. Here p_n=0 means no normal tissue is considered in the FMD optimization algorithm, i.e., $w_n = 0$ and $w_s = w_t = 1$. Although statistic indices for the target volume in the case of p_n=0 are better than others, the average dose of 52.6 dose units and the standard deviation of 33.8 dose units for the normal tissue far exceed the upper limit of 60 dose units. The data listed in Tab. 1 shows that the optimal balance between objectives of high target dose and low normal tissue dose is achieved when p_n=25 dose units. Figure 6 shows corresponding dose-volume histograms for the target volume (Fig. 6(a)), the sensitive organs (Fig. 6(b)) and the normal tissue (Fig.6(c)). The improvement of performance is evident with the optimization of normal tissue dose prescription.

C.3.1.2. Comparison of FIP and HIP methods

The case described above, with a normal tissue dose prescription of 25 units, can be considered an optimal result for the FIP algorithm. In this section the result obtained by the FIP method is compared to that obtained by the hard inverse planning (HIP) method. HIP means that only FMD algorithm, as discussed in Section II, is applied. For the HIP method, two extreme prescriptions are selected: (a) no normal tissue is considered in the optimization algorithm, i.e., $w_n = 0$ and $w_s = w_t = 1$; (b) the prescribed normal tissue dose is fixed, i.e., $p_n = P_n = 60$ and $w_s = w_t = w_n = 1$.

Dose-volume histograms are calculated and illustrated in Fig. 7(a) for the target volume obtained using FIP, HIP(a), and HIP(b), respectively. Corresponding dose-volume histograms for the sensitive organs and the normal tissue are illustrated in Fig. 7(b) and Fig. 7(c). Table 2 provides the relevant statistical parameters. It has been shown that the overall results obtained by optimizing prescription of normal tissue dose (FIP method) are better than those obtained by HIP(a) and HIP(b).

C.3.1.3. Effect of parameter K

As discussed in Section III, validity function $g(\cdot)$ is considered to be adequate if $K \geq 1$. The effect of the parameter K in Eq.(10) on the performance of FIP method is evaluated by using values of $K = 1,2,...,5$. Dose-volume histograms obtained using different K values for the target volume (Fig. 8(a)), the sensitive organs (Fig. 8(b)), and the normal tissue (Fig.8(c)) are calculated and compared. Results indicated that the uniformity of dose for the target volume is improved as K increases. At the same time, the control of dose for the sensitive organ is stronger as K increases. However, the control of dose for the normal tissue is weaker as K increases. Therefore, the result of $K = 5$ is more desirable than those of others are. If K is greater than 5, the performance of normal tissue would be less desirable despite of dose improvement in other structures.

C.3.2. Case 2

The central slice of the phantom geometry in Example 2 is illustrated in Fig.9. Similar to Example 1, seven fan beams are arranged at 0, $2\pi/7$, $4\pi/7$, $6\pi/7$, $8\pi/7$, $10\pi/7$, and $12\pi/7$, respectively. The prescribed doses were set: 100 dose units for the target volume, 20 dose units for the sensitive organs and the upper limit dose of 60 dose units for the normal tissue. The other parameters were L=100 and K=5.

Figure 10 shows dose-volume histograms obtained by using FIP, HIP(a) and HIP(b) methods for the example 2. Figure 10(a) corresponds to the target volume, Fig.10(b) to the sensitive organs, and Fig.10(c) to the normal tissue. Table 3 indicates the relevant statistical parameters: means, standard deviations for the three structures in Example 2. The performance patterns of the FIP algorithm in Example 2 is consistent with the results obtained in Example 1. However, the optimal normal tissue value p_n here is equal to 30. Note that in this example one may also obtain a desirable result without considering normal tissue, i.e., FIP has similar result as HIP(a).

C.4. Meavoltage CT image using limited number of projections

We investigated using a fluorescent/CCD-based EPID, coupled with a novel Multilevel Scheme Algebraic Reconstruction Technique (MLS-ART), for a feasibility study of portal CT reconstruction (Ying 1990, Wong 1990, Yin 1994, Zhu 1995). We used an EPID, set it to work at the linear dynamic range and collimated 6 MV photons from a linear accelerator to a slit beam of 1 cm wide and 25 cm long. We performed scans under a total of 200 MUs for several phantoms in which we varied the number of projections and the MUs per projection. The reconstructed images demonstrated that using the new MLS-ART technique, megavoltage portal CT with a total of 200 MUs can achieve a contrast detectibility of ~2.5% for an object of size 5mm x 5mm and a spatial resolution of 2.5 cm.

We reported our investigation using a CsI(Tl) transparent scintillator x-ray detector together with the multi-level scheme algebraic reconstruction technique (MLS-ART) for megavoltage computed tomography (CT) reconstructions. The reconstructed CT images may be useful for positional verification in radiotherapy. The CsI(Tl) imaging system consists of a scintillator screen coupled to a liquid-nitrogen-cooled slow-scan CCD-TV camera. This system provides better contrast resolution than the standard electronic portal imaging system (EPID), which is especially useful given the low number of projections we are aiming at. The geometry of the imaging system has also been optimized to achieve high spatial resolution (1 lp/mm) in spite of the thickness of the screen. We present the images reconstructed using a pediatric head phantom using a total of 99 projections, and a combined phantom using 50 projections. Image reconstruction was carried out using the MLS-ART technique. We also present the CT images obtained using the back projection technique for comparison purposes. The detectibility?

In addition, we also investigated the use of the kinestatic charge detector (KCD) combined with the multi-level scheme algebraic reconstruction technique (MLS-ART) for x-ray computer tomography (CT) reconstruction. The KCD offers excellent detective quantum efficiency and contrast resolution. These characteristics are especially helpful for applications in which a limited number of projections are used. In addition, the MLS-ART algorithm offers better contrast resolution than does the conventional convolution backprojection (CBP) technique when the

number of projections is limited. Here we present images of a Rando head phantom that was reconstructed by using the KCD and MLS-ART. We also present, for comparison, the images reconstructed by using the CBP technique. The combination of MLS-ART and the KCD yielded satisfactory images after just one or two iterations.

The advantages of MLS-ART applied to conformal radiotherapy are following:

a. The MLS-ART outperforms the conventional CBP technique for low contrast detection given a limited number of projections and it is especially useful for megavoltage CT reconstruction since in radiotherapy we cannot rotate the linear accelerator gantry to acquire a large number of projections in a reasonably short of time. Contrast detectibility is strongly dose-dependent, and for some situations in x-ray imaging, high contrast resolution is not as important as the ability to provide excellent image contrast (Yaffe and Rowlands 1997). Such is the case with megavoltage CT imaging for radiation treatment verification. The high-energy x-ray photons experience inherently low attenuation in tissues. In addition, attenuation of radiation by tissues in this energy range is mainly due to Compton scattering that depends on electron density but not the atomic number. The two factors combined resulted in poor differentiation between various tissues (Johns and Cunningham 1983). Further, the detective quantum efficiency (DQE) of current megavoltage imaging devices is at least one order lower than those of detector for diagnostic x-ray CT. Therefore, megavoltage portal CT requires an efficeint reconstruction technique like the MLS-ART, especially the one that is optimal for situations of low-contrast detectibility. Better contrast detectibility also helps for more accurate dose reconstruction since spatial resolution imposed on dose is even more relaxed.

b. MLS-ART can be used for CT reconstruction using the radiation treatment beams in addition to the regular CT projection beams. Such a 2-step reconstruction will produce much better reconstruction accuracy than simply using the treatment beams themselves because the latter is a case of incomplete data (although even for this case, MLS-ART itself works better than CBP.) In this way, the patient position can be directly and continuously monitored and even corrected during the treatment.

c. Doing conformal radiotherapy using intensity modulated beams and portal CT is complicated by the tumor irregularity. Depending on the target shapes and sparing of critical organs, select treatment beam orientations to be orthogonal or close to orthogonal are important. These orientations must yield small geometrical correlations (less dose overlap) and most complementary dose distribution information. If possible, we could select the beam orientations following the MLS ordering, or in combination with the methods used by [Gokhale, Soderstrom, Bortfeld].

d. MLS-ART might be possible for dose reconstruction. It might be more accurate than the analytical method given a limited number of beams because for any analytical dose integration method, there is an implicit assumption that an infinite number of projections were used. But the integration method would fail if the angles between beams are large unless special techniques like arc therapy or tomotherapy are used.

C.5. Reconstruction of IMRT beams for dose distribution

D. EXPERIMENTAL DESIGN AND METHODS:

D.1. Inverse treatment planning algorithm for IMRT:

Aim 1.1: to develop a fast monotonic descent method for optimization of intensity modulated beams

Aim 1.2: to develop a fuzzy function to represent vague prescription in inverse treatment planning method

Time table:

Year one: Modeling of fuzzy function for vague prescription. Test of its effectiveness using three phantom cases: brain, pelvic, and head and neck.

Year two: Implementation of inverse planning method into clinical practice.

Year three: Test of inverse planning method with real clinical cases.

D.1.1. Research method:

First, it should been pointed out that the definition of fuzzy weight function as shown in Eq. (10) is not a unique form. Different functions may be used to achieve different goals. We tested Gaussian function instead of Eq. (10) and found that the result obtained using Eq.(10) is better than that obtained using a Gaussian function. Second, in this study two loss functions are introduced. One is the objective function as shown in Eq. (8) and the other is the validity function as shown in Eq. (11). The former is used to optimize beam intensity. The latter is employed to evaluate the prescription of normal tissue. Note that the objective function as shown in Eq. (8) cannot replace the validity function as shown in Eq. (11). For example, it is equal important in terms of loss value when the calculated dose in normal tissue is either 10 below or 10 above the prescribed dose. Therefore, Eq.(8) does not completely express the objectives of radiotherapy, and a validity function as shown in Eq.(11) is necessary. In addition, it is clear that Eq.(11) is an unbiased measure function since the loss for the non-target volume is calculated from zero.

In this study we described a fuzzy inverse planning (FIP) method for solving the problem of uncertain prescription optimization in radiation therapy. This study concerned only with the optimization of normal tissue prescription. The dose prescription in the sensitive organs is fixed. Typically, the upper limit dose for the sensitive organ is less than that for the normal tissue. It is difficult to control the calculated dose less than the upper limit for the sensitive organ (except for those cases in which the sensitive organs are far from the target volume). Typically, the mean dose in the sensitive organs is greater than the upper limit dose. Note that, we assume that the importance of matching the calculated dose and the prescribed dose for the target volume is equal to that for the sensitive organ, i.e., $w_t = w_s = 1$. Clinically, it means that the importance of protecting the sensitive organ is the same as that of controlling the tumor. However, different

weighting factors may be chosen by radiation oncologists for a specific clinical case to fulfill a special objective.

A fuzzy inverse treatment-planning algorithm has been developed. This method provides an alternative to soft optimization for treatment planning. The main advantages have two folds. (a) The developed FMD has the fastest convergence speed in the stage of optimizing the beam intensity and the algorithm is simple to use in which no parameter is problem-specific. And (b) the FIP technique can use uncertain information in inverse treatment planning to achieve the optimal balance between the objectives of matching the calculated dose and the prescribed dose for the target volume and minimizing the dose in normal tissue. The presented technique optimizes not only beam intensity distribution but also normal tissue prescription. The performance of the new algorithm has been compared to that of the hard inverse planning methods for two treatment geometries. The calculation time is less than 2 minutes on PC machine (333mHz, 64MB RAM) for 10 slices with a matrix size of 256x256. At the present, it is difficult to compare between different approaches due to difference in test cases, dose calculation and other factors. It would be useful to unify the test geometry and to compare different methods in the future.

D.1.1.1. Objective function

Inverse planning method involves two key components: objective function to define the goal for the optimization, and optimization method to find the optimal solution for a given objective function.

There are two categories of objective function: physical and biological. Since there are not enough clinical data to support most of biological models for TCP/NTCP, this study will continue to use an objective function based on physical models. The constraints for physical objective function involve dose uniformity and dose-volume requirements. We will use the quadratic model as described in the preliminary studies for establishing optimization objection. An analytical study indicated that some biological models could be approximated as a quadratic format (Ref.?). Therefore, the optimization algorithm developed here may be also applicable to resolve objective functions based on biological model.

$$f(\mathbf{x}) = \sum_i \sum_j \sum_k w_{ijk}(P_{ijk} - D_{ijk})^2$$

The physical meaning of w_{ijk}, P_{ijk}, and D_{ijk} are as described in the preliminary studies.

D.1.1.2. Optimization method

The new iteration method, fast-monotonic descent (FMD) method as described in the preliminary studies has shown to be an very efficient approach. Therefore, we will continue to use this method for the optimization of intensity-modulated beams.

Compared to some existing iteration techniques, there are several unique characteristics of FMD technique. (1) The key parameter, step-length, used in update scheme is analytically calculated so that no trial-and-error is involved. Choice of update scheme is critical for fast

convergence and optimal results. Inappropriate selection of the step-length may lead to poor convergence or even none convergence.. (2) Fast and monotonically convergence guarantees the global minimum of the optimization algorithm. (3) The problem of negative beam intensities is effectively eliminated. (4) The algorithm is simple to understand and implement for clinical applications.

D.1.1.3. Fuzzy representation of vague prescription

The concept for a logistic plan is to deliver full dose to the target region while keeping the dose below the maximum tolerance for normal tissues. The proposed quadratic model in the above section is not sufficient to address the upper limits for normal tissue prescription. A fuzzy function will be introduced to represent vague normal tissue prescription.

The theory of fuzzy set is a mathematical tool used to represent uncertain or partial knowledge. In inverse treatment planning, one only knows the upper limits for normal structures but is not certain what is the optimal prescription, especially the prescription for normal tissue and critical organs. Therefore, this category of problem can be represented by the theory of fuzzy set. We will develop an appropriate fuzzy function to represent vague or uncertain knowledge.

The objective function will be divided into three terms. The first term relates to the target volume that is expected to receive uniform prescription dose. The second term relates to the critical organs that are sensitive to radiation damage and a tolerance dose will be set. The third term relates to the normal tissues except critical organs in which dose is expected to be as low as possible. To achieve these goals, the weight factors in the objective function will be redefined as following:

w_{ijk} in target volume $w_t = tt$, where tt is a constant and is used to indicate the importance of matching target dose. Typically, tt=1.

w_{ijk} in critical organs $w_c = cc * h(p_c,P_c)$, where cc is a constant and is used to indicate the importance of matching prescription for each critical organ.

w_{ijk} in critical organs $w_n = nn * g(p_n,P_n)$, where nn is a constant and is used to indicate the importance of matching prescription for normal tissues.

Here both g and h are two fuzzy functions. The fundamental of constructing a fuzzy function is to find proper weighting factors in the objective functions. Linguistically, the closer the prescribed dose is to the tolerance dose, the greater the importance of the lose (i.e., the difference between the tolerance dose and the prescribed dose) is. Mathematically, it may be described by a following function:

$$g(p_n) = \left(\frac{p_n}{P_n}\right)^K, \qquad 0 \le p_n \le P_n \qquad (10)$$

$$h(p_c) = \left(\frac{p_c}{P_c}\right)^K, \qquad 0 \le p_c \le P_c \qquad (10)$$

where K is a positive constant that controls the patterns of $g(\cdot)$ and $h(\cdot)$. These functions are shown in Fig.1. Obviously, any function with a K value of equal to or greater than 1 can be selected to express the mathematical meaning of the following linguistic prescription. Both exponential and Gaussian function will be examined for this purpose.

D.1.1.3. Penalty of optimization method

Fuzzy inverse planning allows many feasible solutions to occur for a specific clinic problem. Selection of a specific treatment plan is determined by evaluating planning validity. Note that Eq. (8) cannot be served as a validity function since the objective of radiation therapy optimization for non-target volume cannot be expressed by a quadratic function. For example, when the calculated dose is greater than (but closer to) the prescribed dose, the objective function will not able to penalize such a situation. To measure the validity of radiation treatment, we introduce a validity function, say $v(\{P_{ijk}\};\mathbf{x})$, which is written as

$$\sum v(\{P_{ijk}\};\mathbf{x}) = tt \sum_{i,j,k\in\Omega_t} \left|P_{ijk} - D_{ijk}\right| + nn \sum_{i,j,k\notin\Omega_t} D_{ijk} + cc \sum_{i,j,k\notin\Omega_t} D_{ijk} \quad (11)$$

The importance of requiring the quadratic function is that it is proved that the global minimum is exist and is unique. Here tt, nn, and cc are used to indicate the importance of matching each term. These parameters may be determined by the planner based on the clinical needs for each individual patient. When an equal importance is reached, tt, nn, and cc are equal to 1. If DVH is used to judge the results, tt, nn, and cc can be used changed to reach final plan.

D.1.2. Evaluation of inverse planning method:

D.1.2.1. Phantom test

We will test the developed inverse planning method with three cylindrical phantoms: brain, head and neck, and pelvis. Each geometry has both complicated target volume and critical organs around it. Clinical applications: based on the information available here, we will try to use step-and-shot technique to deliver the radiation.

Several measures will be calculated for quantitative evaluation of each test:

Dose volume histogram
Statistical data: mean, standard deviation, minimum, and maximum.

Initially, we will use primary beam only for the dose calculation. Beam divergence will be considered and inverse square law will also be applied. The primary beam is acquired from TMR data for 4x4 cm field size of 6 MV photon beam.

D.1.2.2. Patient case test

D.1.2.2. IMRT experiment

Clinical implementation will based on step-and-shot approach.

a. patient CT image
b. input to Pinnacle 3-D planning systme
c. contour target and critical structure and external edges
d. export contours and CT images to inverse planning algorithm
e. generate IMRT intensities for each beam
f. segment each beam for step-and-shot
g. import segmented field to Pinnacle 3-D system
h. calculate MUs for each segment

D.2. Three-dimensional reconstruction of dose distribution

Aim 2.1 to develop a megavoltage CT reconstruction device
Aim 2.2 to develop a dose reconstruction based on limited IMRT radiation beams.

d.2.1 Research method

d.2.1.1
d.2.1.2

d.2.2 Research design

d.2.2.1
d.2.2.2

Time table:

first year:

second year:

third year:

With the patient at the treatment position, we will use the same projection data for the geometry reconstruction to estimate the true dose delivered to the patient. We will develop a scheme for 3-D dose verification, which requires overlaying the reconstructed patient geometry at treatment with the distribution of the delivered dose. This will serve as a verification tool to the initial treatment planning. Any major discrepancy may warrant modification of the patient setup and/or the treatment strategy.

In the current megavoltage CT imaging, we used uniform beam for both the calibration runs and the projection measurements. For the IMRT, the x-ray beam from each projection will be modulated in intensity, i.e., non-uniform. Therefore, we need to measure the IMRT beams before the patient is placed in the treatment room to get the entrance intensity distribution. An alternative way is to down-load this distribution from the IMRT delivery files; however, this option is less direct than measurement. Without these entrance beam intensity, we would be unable to decide whether any exit intensity change is due to the entrance intensity change or different attenuation within the patient geometry. Image reconstructions using the intensity modulated beam can be tested initially using simply compensator or wedge.

We plan to use different patient dose calculation methods based on the measured transmission x-rays (most of the detected x-rays are primary components for that there is a ~50 cm air gap between the patient exit surface and the detector. The scatter fraction for a 20x20 field size, 17 cm thick water and 30 cm air-gap is 10% [Jaffray et al., 1994]). The first two methods are based on the primary photon fluences at the point of dose calculation. We call them the convolution-superposition and the superposition-convolution method. In the first method, the x-ray fluence at the detector surface is ray-traced back to inside the patient's geometry. We convolve the fluence inside the patient with an appropriate energy deposition kernel (dose spread array) to obtain the dose distribution. By superimposing all the distributions over the reconstructed patient geometry, we can obtain the total dose distribution. In the second method, first, the x-ray fluences of all the beams at the detector surface are ray traced back and superimposed together to get the total primary x-ray fluence distribution inside the patient. Then we convolve this total fluence distribution with a rotation dose spread kernel to get the total dose distribution. In both methods, normalization (calibration) is needed. The third method is based on the primary photon distribution attenuated inside the patient. The overall primary attenuation distribution in the patient, which is different from the total primary fluence ray traced back from the detected x-rays, may also be reconstructed, using the similar methods for the emission tomographic reconstructions such as PET and SPECT. (For each beam the attenuation profile is obtained by subtracting the penetrated primary from the entrance beam.) Then we convolve this overall attenuation distribution with a special rotation dose kernel (which is calculated based on the photon numbers rather than the photon fluence) to get the dose distribution. MLS-ART may be applied for such a photon attenuation reconstruction (with some modification) based on the experiences of Herman [1993], but not the conventional CBP technique due to the limited beam numbers. Further, the inhomogeneity corrections can be directly calculated based on the geometric reconstructions. Compared to the first two methods, the 3rd method may be more direct, accurate and convenient. It is also easier for the intensity modulated beams. With faster and growing computation technology including hardware specifically designed for MLS-ART and FFT, we may achieve faster and more accurate on-line verification.

To be more accurate, we need to calculate the primary fluence on the detector's surface by deconvolving the projection data (measured during treatment session, therefore no additional dose to the patient) using the "EPID kernel" (the point spread function of EPID).

We can also use some portal dosimetry methods to model the exit dose distribution and to compare it to the calculation results. We can also use it to model the absorbed dose inside the treatment volume (actually the dose along the beam path) based on the treatment geometry as reconstructed using the MLS-ART. We will compare our results to some other dose modeling and

verification methods such as the portal dose imaging (PDI) technique [Wong et al., 1990], the superposition/convolution method [McNutt et al., 1996a & b], and the inverse filtered (convolution) back-projection method of Holmes and Mackie [1994].

The other advantage of using the CsI(Tl) detector for dose modeling and verification throughout the treatment volume is that compare to commercial EPID which overresponse to low energy x-rays for dosimetry studies, this detector is more tissue equivalent. If we use the a-Si detector, a more active way to reduce over-response is to use organic scintillators (low-Z plastic materials) on the detector so that detector response will be more tissue equivalent. One way is to use a low-Z screen with a buildup phantom such as the solid water. Then the photons undergo interactions in the buildup material. The secondary electrons are mainly absorbed in the organic screen, and the visible photons are emitted toward the a-Si photodiode sensor. The merit of using such an organic screen is that the dose deposition by electrons inside the tissue can be exactly modeled by using the tissue-equivalent organic material. This new screen needs to be fabricated by a medical imaging company because that the currently available screen has poor surface smoothness.

For clinical application of megavoltage portal CT, improving the accuracy of reconstruction rests on more efficient detectors and optimized reconstruction algorithms to most effectively use the available dose. In this proposal, three interrelated specific aims will be perused.

(1) Adapt an efficient x-ray detector to carry out this project. We have 3 options: a) Using Varian Portal Vision Electronic Portal Imaging Device (EPID), which tested to be the best commercial EPID system. b) Using the amorphous silicon system. Varian would lease us a piece of the detector for research purpose for 3 months. c) Collaborate with Herber Zeman's group in the University of Tennessee, Memphis to use their CsI(Tl) CCD system which was specifically designed for megavoltage imaging. This CsI(Tl) system is one of the best megavoltage imaging system providing both good contrast and spatial resolution.

(2) Image reconstruction.. We will use the MLS-ART technique for this specific application, in which we first use a limited number of cone beam projections (dosage close to that in diagnostic CT) to get megavoltage CT reconstruction for patient geometry. Then we will use the treatment beams to further modify the reconstruction. This two-step reconstruction has three important purposes: 1. the second stage will locally improve the CT image quality inside the tumor; 2. The second stage would also let us know the placement of treatment beams inside the patient geometry obtained by the first step. 3. The treatment (dose covered) area can be visualized from the final CT images. MLS-ART can easily perform this 2-step reconstruction. However, it is impossible for the conventional convolution backprojection (CBP) technique.

(3) Dose reconstruction and verification. From the portal image taken at the treatment portal, we could obtain the portal (transit) dosimetry and convert this portal dose information to photon fluence. We then trace this fluence back to the patient and get the fluence inside the target. We then use the convolution-superposition or superposition-convolution or other methods to calculate the dose inside the patient use the fluence. Such a 3D dose distribution can be overlaid onto the patient geometry to verify the treatment plan. Any major discrepancy between the prescribed and actual dose can be corrected by modification of the treatment setup.

In first step, we will test Aim (2) (image reconstruction) based on the work Huaiqun Guan already did (2 projects) on megavoltage CT reconstruction using the Philips SRI-100 system and the CsI-CCD system. We will test Aim (3) using computer simulation.

B. HUMAN SUBJECTS:

No human subject will be used in this study.

C. VERTEBRATE ANIMALS:

No animals will be used in this study.

D. CONSULTANTS:

No consultant will be required.

E. CONSORTIUM ARRANGEMENTS:

No consortium will be arranged.

F. LITERATURE CITED:

4. Yin FF. Rubin P. Schell MC. Wynn R. Raubertas RF. Uschold G. Sandhu A. Nelson DF. An observer study for direct comparison of clinical efficacy of electronic to film portal images. *International Journal of Radiation Oncology, Biology, Physics. 35(5):985-91, 1996 Jul 15.*

6. Yin FF. Schell MC. Rubin P. A technique of automating compensator design for lung inhomogeneity correction using an electron portal imaging device. *Medical Physics. 21(11):1729-32, 1994 Nov.*

7. Yin FF. Schell MC. Rubin P. Input/output characteristics of a matrix ion-chamber electronic portal imaging device. *Medical Physics. 21(9):1447-54, 1994 Sep.*

1. H. Guan and R. Gordon, Computed tomography using ART with different projection access schemes - a comparison study under practical situations, Phys. in Med. and Biol., 41, 1727-43, 1996.

2. H. Guan and R. Gordon, A projection access order for speedy convergence of algebraic reconstruction techniques (ART): A multilevel scheme (MLS) for computed tomography, Phys. in Med. and Biol., 39, 2005-2022, 1994.

3. H. Guan, R. Gordon and Y. Zhu, Combining various projection access schemes with the algebraic reconstruction technique for low-contrast detection in computed tomography, Phys. Med. and Biol. 43, 2413-2421, 1998..

5. H. Guan and Y. Zhu, Megavoltage computed tomography (CT) using a multilevel scheme algebraic reconstruction technique (MLS-ART) and an electronic portal imaging device (EPID), 43, 2925-2937, Phys. Med. and Biol, 1998.

6. H. Guan, M. W. Gaber, F. A. DiBianca and Y. Zhu, CT reconstruction using MLS-ART technique and the KCD imaging system: I. Low energy x-ray studies, IEEE Trans. Med. Imag., 355-358, 1999.

7. H. Guan, Y. Zhu, M. W. Gaber, A. Sawant and H. Zeman, Portal CT reconstruction using the CsI(Tl) transparent scintillator x-ray detector and the MLS-ART technique, Proceeding of the SPIE medical imaging 3336, 716-723, San Diego, CA, 1999.

Antonuk, L.E., Yorkston, J., Huang, W., Sandler, H., Siewerdsen, J.H. and El-Mohri, Y. "Megavoltage imaging with a large-area, flat-panel, amorphous silicon imager," Int. J. Radiation Oncology Biol. Phys. 36, 661-672, 1996.

Bortfeld T. and Schlegel W. , "Optimization of beam orientations in radiation therapy: some theoretical considerations", Phys. Med. Biol. 38, 291-304, 1993.

Boyer, A.L., Antonuk, L., Fenster, A., Van Herk, M., Meertens, H., Munro, P., Reinstein, L.E., & Wong, J. "A review of electronic portal imaging devices (EPIDs)," Med. Phys. 19, 1-16, 1992.

Brahme A., Lind, B. and Nafstadius, P., "Radiotherapeutic computed tomography with scanned photon beams," International Journal of Radiation Oncology Biology Physics 13, 95-101, 1987.

Clinthorne, N.H., "Are hydrogenated amorphous silicon array usable for tomographic imaging?" IEEE Trans. Nucl. Sci. 41, 1517-1521, 1994.

Gokhale, P. and Mussein, E. M. A., "Determination of beam orientation in radiotherapy planning," Med. Phys. 21, 393-400, 1994.

Hansen, V.N., Evans, P.M. & Swindell, W. "Transit dosimetry - computer generated dose images for verification," Proceedings of the XIth International Conference on the Computers in Radiation Therapy, 116-117 (Manchester), 1994.

Heijmen, B.J.M., Pasma, K.L., Kroonwijk, M., Althof, V.G.M., de Boer, J.C.J., Visser, A.G. and Huizenga, H. "Portal dose measurement in radiotherapy using an electronic portal imaging device (EPID)," Phys. Med. Biol. 40, 1943-1955, 1995.

Holmes, T. W. and Mackie, T. R., "A filtered backprojection dose calculation method for inverse treatment planning," Med. Phys. 21, 303-314, 1994.

Jaffray, D. A., Battista, J. J., Fenster, A. and Munro, P., "X-ray scatter in megavoltage transmission radiography: physical characteristics and influence on image quality," Med. Phys. 21, 45-60, 1994.

Kirby, M.C. & Williams, P.C. "The use of an electronic portal imaging device for exit dosimetry and quality control measurements," Int. J. Radiation Oncology Biol. Phys., 31, 593-603, 1995..

Lewis, D.G., Swindell, W., Morton, E., Evans, P. and Xiao, Z.R. "A megavoltage CT scanner for radiotherapy verification," Phys. Med. Biol. 37, 1985-1999, 1992.

Mackie, T. R., "Tomotherapy: A new concept for the delivery of dynamic conformal radiotherapy," Med. Phys. 20, 1709-1719, 1993.

McNutt, T. R., Mackie, T. R., Reckwerdt, P. and Paliwal, B. R., "Modeling dose distributions from portal dose images using the convolution/superposition method," Med. Phys. 23, 1381-1392, 1996.

McNutt, T. R., Mackie, T. R., Reckwerdt, P., Papanikolaou, N. and Paliwal, B. R., "Calculation of portal dose using the convolution / superposition method," Med. Phys. 23, 527-535, 1996.

Munro, P., "Portal imaging technology: Past, present and future," Seminars in Radiation Oncology 5, 115-133, 1995.

Nakagawa, K., Aoki, Y., Akanuma, A., Onogi, Y., Karasawa, K., Terahara, A., Hasezawa, K. and Sasaki, Y., "Development of a megavoltage CT scanner using linear accelerator treatment beam," J. Japan. Soc. Therap. Radiol. Oncol. 3, 265-276, 1991..

Siewerdsen, J.H., Antonuk, L.E., El-Mohri, Y., Yorkston, J., Huang, W., Boudry, J.M., and Cunningham, I.A. "Empirical and theoretical investigation of the noise performance of indirect detection, active matrix flat-panel imagers (AMFPIs) for diagnostic radiology," Med. Phys. 24, 71-89, 1997.

Soderstrom, S. and Brahme, A., "Selection of suitable beam orientations in radiation therapy using entropy and Fourier transform measures," Phys. Med. Biol. 37, 911-924, 1992.

Wong, E., Zhu, Y. and van Dyk, J. "Theoretical developments on fast Fourier transform convolution dose calculations in inhomogeneous media," Med. Phys. 23, 1511-1521, 1996.

Wong, J.W. Slessinger, E.D., Hernes, R.E., Offatt, C.J., Roy, T. & Vanuier, M.W., "Portal dose images I: Quantitative treatment plan verification," Int. J. Rad. Onc. biol. Phys, 18, 1455, 1990.

Ying, X.G., Geer, L.Y., & Wong, J.W., "Portal dose images. II. Patient dose estimation," Int. J. Rad. Onc. Biol. Phys. 18, 1465, 1990.

3. Fiorino C. Uleri C. Cattaneo GM. Calandrino R. On-line exit dose profile measurements by a diode linear array. *Physics in Medicine & Biology. 41(8):1291-304, 1996 Aug.*

4. Zhu Y. Jiang XQ. Van Dyk J. Portal dosimetry using a liquid ion chamber matrix: dose response studies. *Medical Physics. 22(7):1101-6, 1995 Jul.*

1. Hesse BM. Spies L. Groh BA. Tomotherapeutic portal imaging for radiation treatment verification. *Physics in Medicine & Biology. 43(12):3607-16, 1998 Dec.*

2. Parsaei H. el-Khatib E. Rajapakshe R. The use of an electronic portal imaging system to measure portal dose and portal dose profiles. *Medical Physics. 25(10):1903-9, 1998 Oct.*

4. Pasma KL. Kroonwijk M. de Boer JC. Visser AG. Heijmen BJ. Accurate portal dose measurement with a fluoroscopic electronic portal imaging device (EPID) for open and wedged beams and dynamic multileaf collimation. *Physics in Medicine & Biology. 43(8):2047-60, 1998 Aug.*

5. Boellaard R. van Herk M. Uiterwaal H. Mijnheer B. First clinical tests using a liquid-filled electronic portal imaging device and a convolution model for the verification of the midplane dose. *Radiotherapy & Oncology. 47(3):303-12, 1998 Jun.*

6. Pasma KL. Heijmen BJ. Kroonwijk M. Visser AG. Portal dose image (PDI) prediction for dosimetric treatment verification in radiotherapy. I. An algorithm for open beams. *Medical Physics. 25(6):830-40, 1998 Jun.*

7. Boellaard R. van Herk M. Uiterwaal H. Mijnheer B. Two-dimensional exit dosimetry using a liquid-filled electronic portal imaging device and a convolution model. *Radiotherapy & Oncology. 44(2):149-57, 1997 Aug.*

10. Heijmen BJ. Pasma KL. Kroonwijk M. Althof VG. de Boer JC. Visser AG. Huizenga H. Portal dose measurement in radiotherapy using an electronic portal imaging device (EPID). *Physics in Medicine & Biology. 40(11):1943-55, 1995 Nov.*

Bortfeld T, Stein J and Preiser K 1997 Clinically Relevant Intensity Modulation Optimization Using Physical Criteria *XII th* 1-4.
Bortfeld T, Urkelbach J, Boesecke R and Schlegel W 1990 Methods of image reconstruction from projections applied to conformation therapy *Phys. Med. Biol.* 35 1423-1434.
Brahme A 1988 Optimization of stationary and moving beam rediation therapy techniques *Radiotherapy Oncology* 12 129-140.
German S and German D 1984 Stochastic relaxation, Gibbs distribution, and Bayesian resoration of images *IEEE Trans. Patt. Anan. Mach. Int.* PAMI-6 721-741.
Gordon R 1994 A tutorial on ART *IEEE Trans. Nucl. Sci.* 29 78-93.
Herman G 1972 Two direct methods for reconstruction pictures from their projections: a comparetive study *Comput. Graph. Image Proces.* 1 123-144.
Holmes T W and Mackie T R 1994 A comparison of three inverse treatment planning algorithms *Phys. Med. Biol* 39 91-106.
Holmes T W, Mackie T R, Simpkin D and Reckwerdt P 1991 A unified approach to the optimization of brachytherapy and external beam therapy *Int. J. Radiat. Oncol. Biol. Phys.* 20 859-873.
Hristov D H and Fallone B G 1997 An active set algorithm for treatment planning optimization *Med. Phys.* 24 (9) 1455-1464.
Morrill M, Lane G, Jacobson G and Rosen I 1991 Treatment planning optimization using constrained simulated annealing *Med. Biol.* 36 1341-1361.
Webb S and Oldham M 1996 A method to study the characteristics of 3D dose distributions created by superposition of many intensity-modulated beams delivered via a slit aperture with multiple absorbing vanes *Phys. Med. Biol.* 41 2135-2153.
Webb S 1991a Optimization by simulated annealing of three-dimensional conformal treatment planning for radiation fields defined by a multileaf collimator *Phys. Med. Biol.* 36 1201-1226.
Webb S 1991b Optimization of conformal radiotherapy dose distributions by simulated annealing: 2. Inclusion of scatter in the 2D technique *Phys. Med. Biol.* 36 1227-1237.
Xing L and Chen G T Y 1996 Iterative methods for inverse treatment planning *Phys. Med. Biol.* 41 2107-2123.

Research Grant Application
Varian Medical Systems, Inc.

1. Describe the questions to be answered by the research. Include a title and an abstract as well as a general background statement similar to the introduction section of a scientific paper on the proposed work. This should include references, especially those of the principal investigator.

Title: Artificial Intelligence-guided Inverse Treatment Planning

Abstract: An artificial intelligence (AI) method, fuzzy logic, is applied to optimize parameters in the inverse treatment planning for intensity-modulated radiation therapy (IMRT). With the capability of fuzzy inference, the parameter modification of the objective function is guided by physician's treatment intention and experience. For the different parameters involving inverse planning, the corresponding fuzzy inference systems (FISs) are developed in order to accomplish the treatment requirement. With the function of fuzzy inference, the efficiency and quality of inverse planning will be substantially improved.

Introduction:

The conventional inverse treatment planning involves optimizing an intensity spectrum by an objective function in order to obtain an ideal dose distribution. Sometimes, the dose distribution calculated by the optimized intensity spectrum might not be the one we expected. It is often resulted by an improper selection of parameters selected in the objective function. As the desired dose distribution can only be achieved by a refined combination of parameters that are usually unknown, it was inevitable for a planner to try different combinations of parameters in order to achieve a desired dose distribution. At present, this process is done by a trial-and-error approach.[1-10] It is not only time-consuming but also difficult to find a desired combination of parameters.

A number of methods have been proposed in recent years in order to tackle this problem.[4,7,12-16] Starkschall[12] proposed an approach that removed the necessity of defining a "best" treatment plan, and incorporated the dose-volume constraints into a system to search for a feasible plan that could satisfy the constraints. If no calculated doses satisfy the treatment goal, the planner will provide a guide about how the dose-volume constraints may be modified to achieve a feasible result. This approach is only applied to the conventional three-dimensional (3D) treatment planning. Wu and Mohan[4] developed an optimization system, which employed both dose- and dose-volume-based objective functions. In their system, the optimal plan is selected by calculating the cost of the objective function, or "plan score" (the lower the score, the better the plan). Xing et al.[13,14] presented a method which employed a second stage evaluation function to compute the differences between the calculated and the ideal dose volume histograms. Based on the results of the evaluation function, the weighting factors in the objective function are adjusted. This procedure is to minimize both the objective and evaluation functions in a round-robin manner. Later, further improvement is achieved by using a

statistical measure called preference function, which is constructed based on the empirical judgment. The problem about the selection of weighting factor still exists because it translated to the problem of how to specify the parameters in the evaluation or preference function. A similar method was also proposed by Wu et al.[15] using a genetic algorithm to optimize the weighting factors and beam weights in the conventional 3D treatment planning. Li and Yin[7] introduced fuzzy logic into the inverse planning system to adjust the weighting factors for normal tissue. The result was promising. However, optimizing the parameters for the target and critical organ were not included in the system. Also, the weighting factors initialized by the fuzzy functions still need to be modified by the trial-and-error approach.

One of the major advantages of IMRT is to spare dose of the critical organ adjacent to the target. When a strict compromise between target dose and critical dose was required, fine-tuning of parameters in the objective function is important and necessary. As the effect of parameters on the output of the inverse planning is uncertain, it is hard to say which combination of parameters is best for the current case. Generally, this decision is made according the priority of organs involved and is individualized. More concerns will pay to the organ with high priority. As the trial-and-error approach can be regarded as a way using empirical knowledge to guide the parameter modification, it can be substitute by existed AI approaches, such as expert system and fuzzy inference system. The main purpose of this research is to use fuzzy interference system to define parameters in the objective function based on treatment intention instead of trial-and-error approach.

Reference:

1. J. Liacer, "Inverse radiation treatment planning using the dynamically penalized likelihood method," Med. Phys. 24,1751-1764 (1997).
2. H. Dimitre and B. Gino, "A continuous penalty function method for inverse treatment planning," Med. Phys. 25,208-223 (1998).
3. P. S. Cho and S. Lee, "Optimization of intensity modulated beams with volume constraints using two methods: Cost function minimization and projections onto convex sets," Med. Phys. 25, 435-443 (1998).
4. Q. Wu and R. Mohan, "Algorithms and functionality of an intensity modulated radiotherapy optimization system," Med. Phys. 27, 701-711 (2000).
5. S. V. Spirou and C.S. Chui, "A gradient inverse planning algorithm with dose-volume constraints," Med. Phys. 25, 321-333 (1998).
6. I. Rosen, R. G. Lane, "Treatment plan optimization using linear programming," Med. Phys. 18, 141-152 (1991).
7. R. P. Li and F. F. Yin, "Optimization of inverse treatment planning using a fuzzy weight function," Med. Phys. 27, 691-700 (2000).
8. H. Yan, F. F. Yin, H. Q. Guan, and J. H. Kim, "The Fuzzy Logic Guided Inverse Treatment Planning," submitted by Med.Phys. 2002.
9. S. Webb, "Optimization of conformal radiotherapy dose distributions by simulated annealing," Phys. Med. Biol. 34, 1349-1370(1989).

10. Y. Liu, F. F. Yin and Q. Gao, "Variation method for inverse treatment," Med. Phys. 26, 356-363 (1999).
11. S. Webb, Intensity-modulated radiation therapy, (Institute of Physics Publishing, Bristol, UK, 2001).
12. G. Starkschall and A. Pollack, "Treatment planning using a dose-volume feasibility search algorithm," Int. J. Rad. Onc. Bio. Phys. 49, 1419-27(2001).
13. L. Xing and J. Li, "Optimization of importance factors in inverse planning," Phys. Med. Biol. 44, 2525-2536 (1999).
14. L. Xing and J. Li, "Estimation theory and model parameter selection for therapeutic treatment plan optimization," Med. Phys. 26, 2348-2358 (1999).
15. X. G. Wu and Y. P. Zhu, "An optimization method for importance factors and beam weights based on genetic algorithms for radiotherapy treatment planning," Phys. Med. Biol. 46,1085-1099, (2001).

2. Who are the principal investigator and co-investigators and what are their qualifications?

PI: Fang-Fang Yin, PH.D., Division Head, Medical Physics

Co-PI: Hui Yan, PH.D., Assistant Staff Investigator

3. What is the benefit of the proposed research to radiation oncology?

(1) The heuristic and practical experience (from physician, physicist, planner) can be used to guide the optimizing the parameters of inverse planning in order to improve the dose distribution;
(2) The conformity of target dose distribution can be improved and high target dose could be feasible – improve the quality of inverse planning;
(3) The time spent on trial-and-error test can be reduced significantly and the planner will be free from this time-consuming task – improve the efficiency of inverse planning.

4. How might the proposed research enhance Varian products?

As the goal of our study is to optimize the parameters used for IMRT, this will improve the calculated dose distribution and then delivery effect using the current Varian Linac and MLC.

5. How much will the research cost Varian?

$100,000

6. Provide a budget showing how the money will be spent.

$75,000 Salary and benefits for a staff investigator
$5,000 for miscellaneous, office supplies, presentation, manuscript, and meeting, etc.
$20000 computer hardware and software

$20000 indirect cost

7. Is there an overhead charge and is the rate negotiable? Varian will pay no more than 25% overhead.

Yes. 25%.

8. Are other resources needed from Varian such as engineering or service support?

Technical support for research software interface between in-house developed and Eclipse IMRT.

9. What other resources and funding are available for this project, or related projects, from your institution and other sources?

Presently none.

Please answer these questions briefly in a Word document and send by email to Richard.morse@varian.com.

Submitted to Medical Physics
Confidential until publication

The Fuzzy Logic Guided Inverse Treatment Planning

Hui Yan, PhD
Fang-Fang Yin, PhD
Huaiqun Guan, PhD
Jae Ho Kim, MD, PhD

Department of Radiation Oncology
Henry Ford Hospital, Detroit, MI 48202

Corresponding address:

Hui Yan, Ph.D.
Department of Radiation Oncology
Henry Ford Hospital
Detroit, MI 48202, USA
Email: hyan1@hfhs.org
Phone: (313)916-3452
Fax: (313)916-3235

Version date: 3/18/2002
Revision date: 12/12/2002

I. INTRODUCTION

Conventional inverse treatment planning involves optimizing the beam intensity spectrum by using an objective function in order to obtain an ideal dose distribution. However, the dose distribution calculated by the optimized intensity spectrum might not be the one we expected. The choices of weighting factors in the objective function have an important impact on the calculated doses. Usually, this kind of tasks is done by a trial-and-error approach based on planner's experience.[1-10] It is not only time-consuming but is also difficult to achieve the expected dose distribution among different organs involved.

A number of methods have been proposed in recent years in order to tackle this problem.[4,7,11-15] Starkschall[11] proposed an approach that removed the necessity of defining a "best" treatment plan, and incorporated the dose-volume constraints into a system to search for a feasible plan that could satisfy the constraints. If no calculated doses satisfy the treatment goal, the planner will provide a guide about how the dose-volume constraints may be modified to achieve a feasible solution. This approach was only applied to the conventional three-dimensional (3D) treatment planning. Wu and Mohan[4] developed an optimization system, which employed both dose- and dose-volume-based objective functions. In their system, the optimal plan was selected by calculating the cost of the objective function, or "plan score" (the lower the score, the better the plan). Xing *et al.*[12, 13] presented a method which employed a second stage evaluation function to compute the differences between the calculated and the ideal dose volume histograms. Based on the results of the evaluation function, the weighting factors

in the objective function were adjusted. This procedure was done to minimize both the objective and evaluation functions in a round-robin manner. An improvement was proposed using a statistical measure called preference function, that was constructed based on the empirical judgment.[13] Further investigation is expected to resolve the problem of how to specify the parameters in the preference function. A similar method was also reported by Wu *et al.*[14] using a genetic algorithm to optimize the weighting factors and beam weights in the conventional 3-D treatment planning. Li and Yin[7] introduced fuzzy logic into the inverse planning system to adjust the weighting factors for normal tissue. The result was promising. However, optimizing the weighting factors for target and critical organs were not included in the system.

As inverse treatment planning plays a key role in IMRT, effectively selecting the parameters for a given objective function becomes a challenging problem. The increasing applications of IMRT has prompted the need for the development of an intelligent technique to guide the optimization of parameters used in inverse planning. As the fuzzy inference system (FIS) is constructed to perform the inference as a human does, it is suitable to solve problems involving parameter optimization in inverse planning.[15] In this study, we developed a fuzzy inference system to guide the optimization of weighting factors in inverse planning. The principle of the fuzzy inference system is introduced in Sec. II. The results with two representative cases (one simulated case and one clinical case) are presented in Sec. III. In Sec. IV, we discuss the strength and capability of this approach.

II. MATERIALS AND METHODS

For a given dose prescription, conventional inverse treatment planning consists of two steps: (1) finding the suitable weighting factors for involved organs and (2) optimizing the intensity spectrum based on the given weighting factors. As there are a large number of choices for weighting factors, finding the desired ones for a given objective function is difficult. In this study, we developed a fuzzy inference system (FIS) to optimize the values of weighting factors and compute the intensity spectrum by the iterative gradient technique. The involved organs in this system are categorized as the target volume (TV), the critical organs (CO), and the normal tissue (NT).

A. The principle of the fuzzy inference system

The flow chart of FIS is illustrated in Fig. 1. It consistes of three main modules, i.e., the Fuzzifier, the Inference Engine (consisted of fuzzy rules) and the Defuzzifier. For each variable input to the fuzzy inference system, a number of fuzzy sets are defined with appropriate membership functions. These membership functions are labeled with linguistic tags frequently used by humans (such as "High" dose). During the process of fuzzification (corresponding to the module of Fuzzyifier), the single input value is compared to the membership functions defined for that input variable. If the membership functions have a non-zero output, it will take effect on the final result of the FIS. Generally, the fuzzifier calculates the response of rules for the input values, and the inference engine modifies the consequent of rules in response to the input values and the

defuzzifier generates final output based on the result of inference engine.

The inputs of this system are defined as the characteristic doses $[C_{TV}, C_{CO}, C_{NT}]$, which consist of the mean dose ($Mean_i$, i =*TV, CO, NT*) and its standard deviation (STD_i, i =*TV, CO, NT*). For the target volume, $C_{TV} = Mean_{TV} - STD_{TV}$. For the critical organs and normal tissue, $C_{CO} = Mean_{CO} + STD_{CO}$ and $C_{NT} = Mean_{NT} + STD_{NT}$. The outputs of FIS $[\Delta W_{TV}, \Delta W_{CO}, \Delta W_{NT}]$ are defined as the adjustment of the weighting factors for each involved organs. For each input variable, two fuzzy sets, "High (H)" and "Low (L)", are defined with membership functions $[f_i^H(x), f_i^L(x), i$ =*TV, CO, NT*], as shown in Figs. 2a-2c. For each output variable, three fuzzy sets, "Increase (I)", "Not change (N)", and "Decrease (D)", are defined with membership functions $[g_i^I(x), g_i^N(x), g_i^D(x), i$ =*TV, CO, NT*]. For the target volume, these three membership functions are shown in Fig. 2d. Similar membership functions are defined for critical organ and normal tissues for the same adjustment strategy and therefore not shown.

Based on the input and output variables defined above, fuzzy rules are established for the fuzzy inference engine. As shown in Appendix I, eight rules are employed in this system. In each rule, the if-part of rule is called antecedent and the then-part of rule is called consequent. Two of them (Rule 5 and Rule 8) are used to demonstrate the procedure of fuzzy inference as shown in Fig. 3. Note that the input (output) variables are labeled using the **bold** fonts and their corresponding linguistic tags are labeled using the *italic* fonts in each rule. According to the linguistic tags, the corresponding

membership functions for the input fuzzification are specified as shown in Step 1 of Fig. 3. Such as the input variable C_{TV}, the membership function f_{TV}^{H} is specified in Rule 5 by the linguistic tag "High". For each rule, the outputs of the fuzzification are $[D_{TV}^{5}, D_{CO}^{5}, D_{NT}^{5}]$ and $[D_{TV}^{8}, D_{CO}^{8}, D_{NT}^{8}]$, respectively. Based on these outputs of fuzzification, the degree of support ($D_{support}$) for each rule is achieved by a logic operator "Min", such as $D_{support}^{5} = \text{Min}(D_{TV}^{5}, D_{CO}^{5}, D_{NT}^{5})$ and $D_{support}^{8} = \text{Min}(D_{TV}^{8}, D_{CO}^{8}, D_{NT}^{8})$, as shown in Step 2 of Fig. 3. Note that the degree of support represents the applicability of rule's antecedent for given inputs. Based on the degree of supports, the fuzzy inference is performed by a standard implication method, which is accomplished by a logic operator "Min". For example in Step 3, the membership function $g_{TV}^{N}(x)$ in Rule 5 is modified as $g_{TV}^{N,D_5}(x) = \text{Min}(D_{support}^{5}, g_{TV}^{N}(x))$. The modified membership functions became $[g_{TV}^{N,D_5}(x), g_{CO}^{N,D_5}(x), g_{NT}^{N,D_5}(x)]$ and $[g_{TV}^{N,D_8}(x), g_{CO}^{I,D_8}(x), g_{NT}^{I,D_8}(x)]$ for Rule 5 and Rule 8, respectively. As there are two sets of modified membership functions obtained, it is necessary to combine them to produce a single one. In Step 4, they were aggregated into one set by a logic operator "Max", i.e., $[\overline{g_{TV}}(x), \overline{g_{CO}}(x), \overline{g_{NT}}(x)] = [\text{Max}(g_{TV}^{N,D_5}(x), g_{TV}^{N,D_8}(x)], \text{Max}(g_{CO}^{N,D_5}(x), g_{CO}^{I,D_8}(x)), \text{Max}(g_{NT}^{N,D_5}(x), g_{NT}^{I,D_8}(x))]$. The aggregated functions represent the combined consequent from all the rules. Finally, the aggregated functions are defuzzified to a single value by the centroid method in Step 5. The x-coordinate of the centroid (represented by sign "⊕") for each aggregated function was the final output, the adjustment amount of weighting factors.

B. The fuzzy logic guided inverse planning algorithm

The flow chart of the FLGIP system is schematically illustrated in Fig. 4. First, the dose prescription and weighting factors are set to their initial values. Then, an iterative gradient algorithm is used to calculate the intensity spectrum **x**. In our study, the objective function is defined as follows:

$$f(\mathbf{x}) = \sum_i \sum_j \sum_k w_{ijk} (p_{ijk} - d_{ijk})^2 , \tag{1}$$

Where $d_{ijk} = \sum_{n=1}^{N} A_{n,ijk} x_n$ is the calculated dose for each voxel, $A_{n,ijk}$ is the relative dose coefficient, or dose per unit intensity of pencil beam. p_{ijk} is the dose prescription and w_{ijk} is the weighting factor defined as follows:

$$p_{ijk} = \begin{cases} P_{TV}, & if \ \ (i,j,k) \in \Omega_{TV} \\ P_{CO}, & if \ \ (i,j,k) \in \Omega_{CO} \\ P_{NT}, & if \ \ (i,j,k) \in \Omega_{NT} \end{cases}, \qquad w_{ijk} = \begin{cases} W_{TV}, & if \ \ (i,j,k) \in \Omega_{TV} \\ W_{CO}, & if \ \ (i,j,k) \in \Omega_{CO} \\ W_{NT}, & if \ \ (i,j,k) \in \Omega_{NT} \end{cases}.$$

Ω_{TV}, Ω_{CO} and Ω_{NT} denotes the target volume, the critical organ volume, and the normal tissue volume, respectively. The minimization of the objective function under the constraint of $x_n \geq 0$ can be written as a problem of

$$\begin{aligned} &\min_{\mathbf{x}} \{f(\mathbf{x})\} \\ &\text{subject to } x_n \geq 0, \forall n. \end{aligned} \tag{2}$$

Eq. 2 can be solved by the fast-monotonic-descent (FMD) method developed by Li and Yin,[7] which is an optimized iterative gradient technique for the quadratic function. Based on the optimized intensity spectrum, the characteristic doses are calculated and then input

to the FIS. Using fuzzy inference, the adjustment amounts of weighting factors $[\Delta W_{TV}, \Delta W_{CO}, \Delta W_{NT}]$ are obtained. Then, the weighing factors for the next iteration are modified as follows

$$W_i(n+1) = W_i(n)[1 + \Delta W] \qquad i \in \{TV, CO, NT\}, \quad \Delta W \in [-1,1]. \tag{3}$$

As the weighting factors affect the output of inverse planning by their relative values rather than the absolute values, they are re-normalized to [0, 1] by the following formula:

$$W_i^*(n+1) = \frac{W_i(n+1)}{\sqrt{W_{TV}(n+1)^2 + W_{CO}(n+1)^2 + W_{NT}(n+1)^2}} \qquad i \in \{TV, CO, NT\}. \tag{4}$$

This updating procedure repeats until the following convergence criterion (5) is satisfied:

$$\frac{\sqrt{[C_{TV}(n+1) - C_{TV}(n)]^2 + [C_{CO}(n+1) - C_{CO}(n)]^2 + [C_{NT}(n+1) - C_{NT}(n)]^2}}{\sqrt{C_{TV}(n)^2 + C_{CO}(n)^2 + C_{NT}(n)^2}} < \mathrm{T}. \tag{5}$$

where T is a small threshold number, such as 0.01.

III. RESULTS

The performance of FLGIP system was examined using two cases (one simulated and one clinical). Dose-volume histograms (DVHs), plus the variation of characteristic doses and weighting factors versus the iteration number, are used as the primary tools to evaluate the performance of this system. Pencil beams of 6 MV were used. For simplicity, the primary-only dose at depth is used in the calculation. The initial weighting factors $[W_{TV}, W_{CO}, W_{NT}]$ are set to [1,1,1] (after re-normalization using formula (4), they became [0.58, 0.58, 0.58]) and the convergence constant T was set to 0.01.

A. The Simulated Case

The central slice of this case is illustrated in Fig. 5a. The layout on this slice simulates the spinal cord with a target volume surrounding it. Seven treatment beams are uniformly arranged between 360 degrees. This configuration is typical in spinal radiosurgery using IMRT.

The FLGIP system was tested using four sets of different dose prescriptions: [100%, 20%, 50%], [100%, 30%, 50%], [100%, 40%, 50%], [100%, 50%, 50%]. Fig. 6 shows the variation of (a) characteristic doses and (b) weighting factors versus the iteration number for dose prescription [100%, 30%, 50%]. The results indicate that for the target volume and critical organ, the characteristic doses monotonically converge to the prescribed doses (the normal tissue dose also converges, but in a much less rate due to its large volume.) The results shown in Table I demonstrate that the high target dose and low critical organ dose are achieved simultaneously and both meet the prescribed ones. Their corresponding DVHs for (a) the target volume, (b) the critical organ, and (c) the normal tissue are shown in Fig. 7. Note that, the final results also depend on the provided dose prescriptions. For each set of dose prescriptions, their corresponding isodose distributions are shown in Fig. 8.

The effect of initial weighting factors on the final characteristic doses was examined by using eight sets of initial values with the same dose prescriptions [100%, 30%, 50%]. The characteristic doses for each set converged within 50 iterations. The final results and

the standard deviations are shown in Table II. The results indicate that the achieved characteristic doses by different sets of initial weighting factors are comparable. We averaged the final eight sets of weighting factors. The mean weighting factors and their standard deviations are 0.139 ± 0.113 for the target volume, 0.985 ± 0.025 for the critical organ, and 0.004 ± 0.003 for the normal tissue. It implies that there could be a limited space for the selection of optimal weighting factors.

B. The Clinical Case

The central slice for this clinical case is illustrated in Fig. 5b. Eleven beams are arranged at 0°, 33°, 66°, 90°, 120°, 150°, 210°, 240°, 270°, 300°, 330°. This configuration represents a complicated IMRT case. The dose prescription is set to [100%, 30%, 50%]. The variations of the characteristic doses and weighting factors versus the iteration number are shown in Fig. 9a and Fig. 9b, respectively. The characteristic dose C_{TV} monotonically converges to its prescribed dose 100% while the characteristic doses C_{CO} and C_{NT} monotonically converges to the doses below their prescribed values, 30% and 50% respectively. The DVHs of the calculated doses for different organs at three iterations 5, 10, 15 are shown in Fig.10. The results indicate that the gap between the DVHs of target volume (Fig. 10a) and critical organs (Fig. 10c) increases with increased iteration number. The substantial improvements of isodose distributions around the critical organ CO_1 (the one closet to target volume) in different iterations can be easily identified from Fig. 11.

IV. DISCUSSIONS

A fuzzy inference system was developed to automatically modify the weighting factors in inverse treatment planning in order to achieve the dose distributions best matching the treatment requirements. The fundamental inference mechanism is demonstrated by a mini system consisted of two rules as shown in Fig. 3. Among the eight rules, Rule 5 plays the primary role to drive the system toward the convergence while Rule 8 (plus the other six rules) drives the inputs toward its prescribed ones. For example, when the inputs for critical organ and normal tissue are much higher than their prescribed doses, the output of FIS will mainly be determined by the adjustment of Rule 8. Once the inputs approach their prescribed ones to better match the antecedent of Rule 5 (usually after several iterations), the consequent of Rule 5 will take more effect on the output of FIS and drive the system towards convergence. Note that, the other six rules in Appendix I are used to process different scenarios of mismatching between characteristic doses and prescribed doses of different organs.

The details of adjustment process are shown in Fig. 6 and Fig. 9. At the first several iterations, the weighting factor for the target volume decreases and the weighting factor for the critical organs increases quickly. After few iterations, as the characteristic doses approach their prescribed ones, the adjustments of weighting factors gradually reduce. It is noteworthy that the characteristic doses for the target and critical organs in the last iteration satisfy their dose prescriptions. For the normal tissue, however, the final

characteristic dose is appreciably lower than its prescribed one due to its large volume. Although some rules seemingly take less effect on or are seldom used in these two cases, these rules are necessary for the more complicated cases. In addition, the results shown in Fig. 7 indicate that using different dose prescriptions could result in different dose distributions. Potentially, the fuzzy inference technique may also be used to optimize other parameters in inverse planning such as the beam orientation, the dose prescription etc. Investigations are still underway for these applications.

As the configuration of FIS is flexible, it provides us a wide space to customize the configuration for different applications. In this system, the input characteristic doses are chosen as the mean dose combined with its standard deviation. For target, the lower than mean input dose will help the FIS to drive the target dose to be higher toward the prescribed one in the next iteration. Similarly, for critical organ and normal tissue, the higher than mean input dose will drive critical and normal tissue doses to be lower toward the prescribed ones in the next iteration. In this way, both high target dose and lower critical organ (and normal tissue) doses may be easier to achieve. For output variables, they are simply defined as the relative adjustment of the weighting factors, which are between -1 and 1. For the selection of inference rules, it is primarily determined by the clinical experience. The general treatment intention may be described as: If the target dose is low, its weighting factor should be increased. If the critical organ and normal tissue doses are high, their weighting factors should be increased. In our system, such treatment intention is expressed by eight rules (Appendix I), which is a complete combination of linguistic tags for three kinds of involved organs. This option

may not be the best but can avoid any unpredicted input values. As for the selection of membership functions, the Gaussian function is adopted due to its simplicity and popularity for most of the engineering applications. In some circumstance, part of the Gaussian function is used, such as those shown in Fig. 2a-2c.

V. CONCLUSION

A fuzzy logic guided inverse planning system has been developed. This system provides an effective and efficient approach to optimize the parameters used in inverse planning. The main advantage of using FIS is that it can perform the sophisticated inference formerly done by trial-and-error approach. Relying on the planner's experience and knowledge on how to compromise parameters among different organs involved, the optimization of weighting factors can be easily accomplished by encoded rules. As demonstrated by the result of two cases, the fuzzy inference system could undertake the very complex task of parameter optimization in inverse planning.

VI. ACKNOWLEDGE

We thank Mrs. Janice freytag for her editorial assistance.

REFERENCES

1. J. Liacer, "Inverse radiation treatment planning using the dynamically penalized likelihood method," Med. Phys. **24**, 1751-1764 (1997).
2. H. Dimitre and B. Gino, "A continuous penalty function method for inverse treatment planning," Med. Phys. **25**, 208-223 (1998).
3. P. S. Cho and S. Lee, "Optimization of intensity modulated beams with volume constraints using two methods: Cost function minimization and projections onto convex sets," Med. Phys. **25**, 435-443 (1998).
4. Q. Wu and R. Mohan, "Algorithms and functionality of an intensity modulated radiotherapy optimization system," Med. Phys. **27**, 701-711 (2000).
5. S. V. Spirou and C.S. Chui, "A gradient inverse planning algorithm with dose-volume constraints," Med. Phys. **25**, 321-333 (1998).
6. I. Rosen, R. G. Lane, "Treatment plan optimization using linear programming," Med. Phys. **18**, 141-152 (1991).
7. R. P. Li and F. F. Yin, "Optimization of inverse treatment planning using a fuzzy weight function," Med. Phys. **27**, 691-700 (2000).
8. S. Webb, "Optimization of conformal radiotherapy dose distributions by simulated annealing," Phys. Med. Biol. **34**, 1349-1370(1989).
9. Y. Liu, F. F. Yin and Q. Gao, "Variation method for inverse treatment," Med. Phys. **26**, 356-363 (1999).
10. S. Webb, *Intensity-modulated radiation therapy*, (Institute of Physics Publishing, Bristol, UK, 2001).
11. G. Starkschall and A. Pollack, "Treatment planning using a dose-volume feasibility

search algorithm," Int. J. Rad. Onc. Bio. Phys. 49, 1419-27(2001).

12. L. Xing and J. Li, "Optimization of importance factors in inverse planning," Phys. Med. Biol. 44, 2525-2536 (1999).

13. L. Xing and J. Li, "Estimation theory and model parameter selection for therapeutic treatment plan optimization," Med. Phys. 26, 2348-2358 (1999).

14. X. G. Wu and Y. P. Zhu, "An optimization method for importance factors and beam weights based on genetic algorithms for radiotherapy treatment planning," Phys. Med. Biol. 46,1085-1099, (2001).

15. L. T. Lin and C. S. G. Lee, *Neural fuzzy systems*, (Prentic-Hall PTR, New Jersey, US 1996).

FIGURE CAPTIONS

Figure 1 Schematic illustration of the fuzzy inference system (FIS) used for modification of the weighting factors.

Figure 2 Illustration of membership functions used in FIS. (a) The membership functions "High" ($f_{TV}^{H}(x)$) and "Low" ($f_{TV}^{L}(x)$) defined for input variable C_{TV}. (b) The membership functions "High" ($f_{CO}^{H}(x)$) and "Low" ($f_{CO}^{L}(x)$) defined for input variable C_{CO}. (c) The membership functions "High" ($f_{NT}^{H}(x)$) and "Low" ($f_{NT}^{L}(x)$) defined for input variable C_{NT}. (d) The membership functions "Decrease" ($g_{TV}^{D}(x)$), "Not change" ($g_{TV}^{N}(x)$), and "Increase" ($g_{TV}^{I}(x)$) defined for the output variable ΔW_{TV}.

Figure 3 Demonstration of the inference procedure by two rules. Step 1: Inputs fuzzification. Step 2: Degree of support. Step 3: Fuzzy inference (implication operation). Step 4: Aggregation operation. Step 5: Output defuzzificaiton.

Figure 4 Flow chart of the fuzzy logic guided inverse treatment planning system.

Figure 5 The central slices for (a) a simulated case and (b) a clinical case. TV, CO and NT represent the target volume, the critical organ and the normal tissue, respectively. Arrows pointed to the target volume indicate the beam directions.

Figure 6 The variations of (a) characteristic doses and (b) weighting factors versus the iteration number in the simulated case for the dose prescription [100%, 30%, 50%]. Note that the initial weighting factors [1,1,1] were normalized to [0.58, 0.58, 0.58] using formula (4).

Figure 7 Dose-volume histograms of the calculated doses in the simulated case for (a) the target volume, (b) the critical organ, and (c) the normal tissue for four sets of dose prescriptions.

Figure 8 The dose distributions in the central slice of simulated case for four sets of dose prescriptions (a) [100%, 20%, 50%], (b) [100%, 30%, 50%], (c) [100%, 40%, 50%], (d) [100%, 50%, 50%].

Figure 9 Variations of (a) characteristic doses and (b) weighting factors versus iteration number in the clinical case for the dose prescription [100%, 30%, 50%]. Note that the initial weighting factors [1,1,1] were normalized to [0.58, 0.58, 0.58] using formula (4).

Figure 10 Dose-volume histograms of calculated dose distributions for five involved organs: (a) the target volume, (b) the normal tissue, (c) the critical organ 1, (d) the critical organ 2, and (e) the critical organ 3 at iteration 5, 10, and 15, respectively.

Figure 11 The dose distributions in the clinical case at (a) Iteration 5, (b) Iteration 10, and (c) Iteration15.

Table II. Comparison of results by using different sets of initial weighting factors.

Weighting factor			Calculated dose (%)					
Target volume	Critical organ	Normal tissue	Target volume		Critical organ		Normal tissue	
			Mean	STD	Mean	STD	Mean	STD
0.1	0.1	0.1	100.8	5.6	30.2	0.8	25.8	18.8
0.1	0.1	1.0	101.0	5.9	30.0	0.2	25.7	19.1
0.1	1.0	0.1	101.1	6.0	30.0	0.2	25.7	19.1
1.0	0.1	0.1	100.3	4.5	30.8	3.0	25.3	18.5
1.0	1.0	1.0	100.8	5.6	30.2	0.8	25.8	18.8
1.0	1.0	0.1	100.5	5.1	30.4	1.5	25.5	18.6
1.0	0.1	1.0	100.4	5.2	30.3	1.3	25.3	18.7
0.1	1.0	1.0	100.7	6.0	30.0	0.1	26.6	22.5

Table I. Comparison of results by using different sets of dose prescriptions.

Dose prescription (%)			Calculated dose (%)					
Target volume	Critical organ	Normal tissue	Target volume		Critical organ		Normal tissue	
			Mean	STD	Mean	STD	Mean	STD
100	20	50	102.1	6.3	20.5	2.4	26.2	18.9
100	30	50	102.3	5.3	31.1	2.1	26.6	19.1
100	40	50	102.3	4.6	40.2	1.8	26.9	18.7
100	50	50	102.4	4.1	50.3	2.0	27.2	18.6

Appendix I. The rules of fuzzy inference system

Rule 1: If C_{TV} is *low* and C_{CO} is *low* and C_{NT} is *low*,
Then W_{TV} will *increase* and W_{CO} will *not change* and W_{NT} will *not change*.

Rule 2: If C_{TV} is *low* and C_{CO} is *low* and C_{NT} is *high*,
Then W_{TV} will *increase* and W_{CO} will not *change* and W_{NT} will *increase*.

Rule 3: If C_{TV} is *low* and C_{CO} is *high* and C_{NT} is *low*,
Then W_{TV} will *increase* and W_{CO} will *increase* and W_{NT} will *not change*.

Rule 4: If C_{TV} is *low* and C_{CO} is high and C_{NT} is *high*,
Then W_{TV} will *increase* and W_{CO} will *increase* and W_{NT} will *not change*.

Rule 5: If C_{TV} is *high* and C_{CO} is *low* and C_{NT} is *low*,
Then W_{TV} will not *change* and W_{CO} will *not change* and W_{NT} will *not change*.

Rule 6: If C_{TV} is *high* and C_{CO} is *low* and C_{NT} is *high*,
Then W_{TV} will not *change* and W_{CO} will *not change* and W_{NT} *increases*.

Rule 7: If C_{TV} is *high* and C_{CO} is *high* and C_{NT} is *low*,
Then W_{TV} will *not change* and W_{CO} will *increase* and W_{NT} will *not change*.

Rule 8: If C_{TV} is *high* and C_{CO} is *high* and C_{NT} is *high*,
Then W_{TV} will *not change* and W_{CO} will *increase* and W_{NT} will *not increase*.

ABSTRACT

An intelligent technique, fuzzy logic, was applied to optimize the weighting factors in the objective function of inverse treatment planning for intensity-modulated radiation therapy (IMRT). Based on this technique, the optimization of weighting factors is guided by the fuzzy rules while the intensity spectrum is optimized by a fast-monotonic-descent method. The resultant fuzzy logic guided inverse planning (FLGIP) system is capable of finding the optimal combination of weighting factors for different anatomical structures involved in treatment planning. This system was tested using one simulated (but clinically relevant) case and one clinical case. The results indicate that the optimal balance between the target volume and the critical organ dose was achieved by a refined combination of weighting factors. With the help of fuzzy inference, the efficiency and effectiveness of inverse planning for IMRT are substantially improved.

Key words: fuzzy logic, optimization, inverse treatment planning, intensity-modulated radiation therapy.

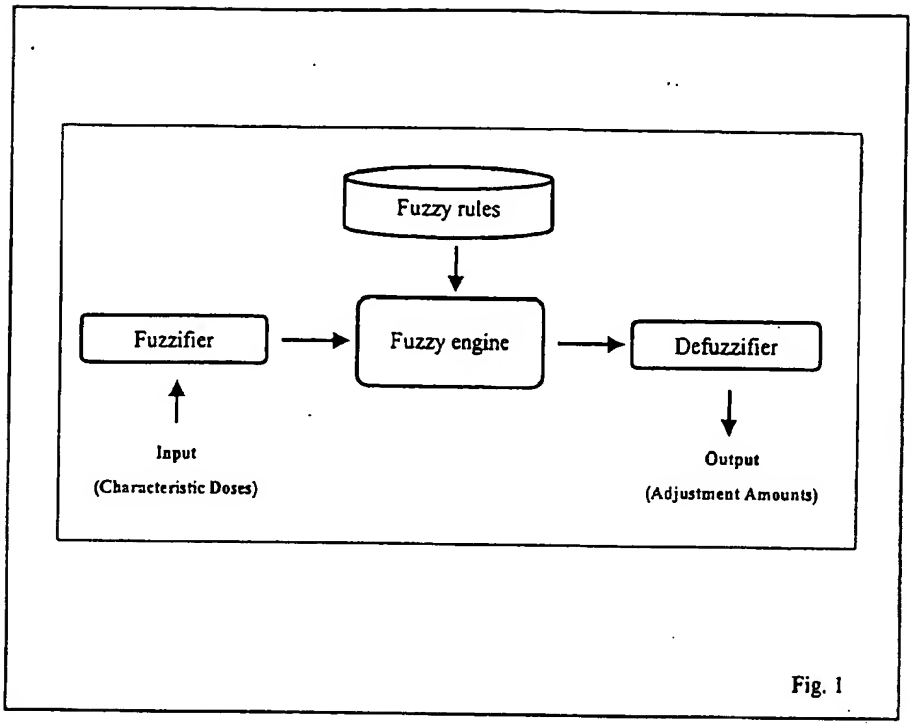
Fuzzy rules
Fuzzifier
Fuzzy engine
Defuzzifier
Input
(Characteristic Doses)
Output
(Adjustment Amounts)

Fig. 1

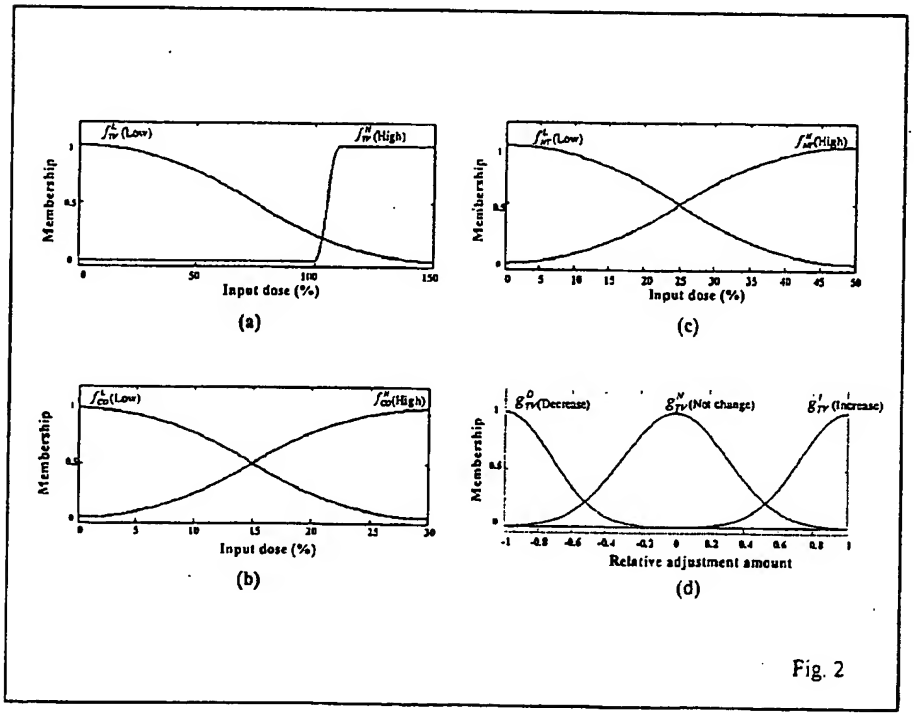
Membership
Input dose (%)
(a)
(c)
(b)
(d)
Relative adjustment amount

Fig. 2

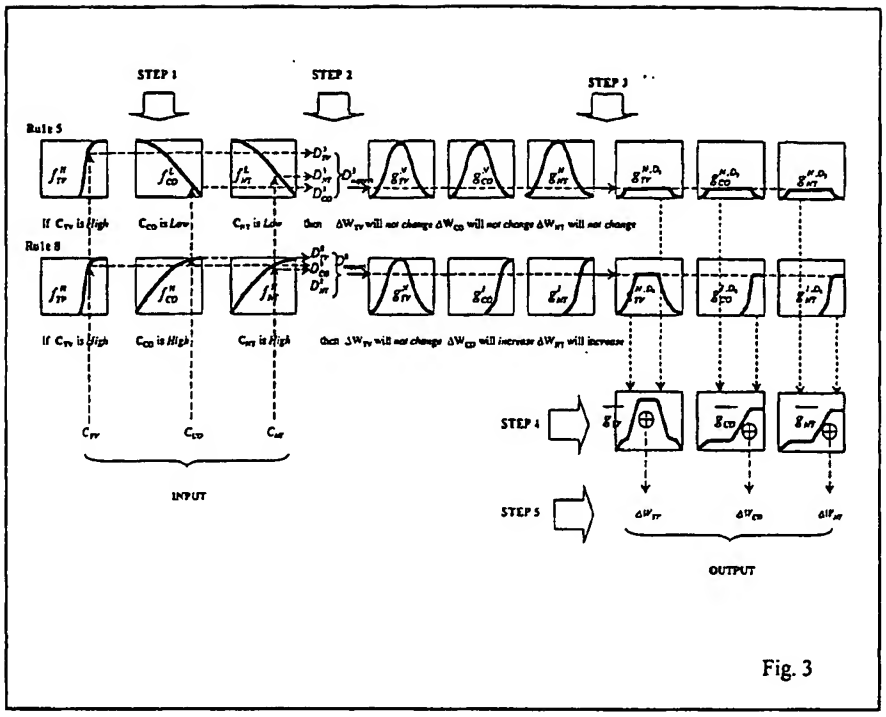
STEP 1
STEP 2
STEP 3
Rule 5
If C_{TV} is High C_{CO} is Low C_{MT} is Low then ΔW_{TV} will not change ΔW_{CO} will not change ΔW_{MT} will not change
Rule 8
If C_{TV} is High C_{CO} is High C_{MT} is High then ΔW_{TV} will not change ΔW_{CO} will increase ΔW_{MT} will increase
STEP 4
STEP 5
INPUT
OUTPUT

Fig. 3

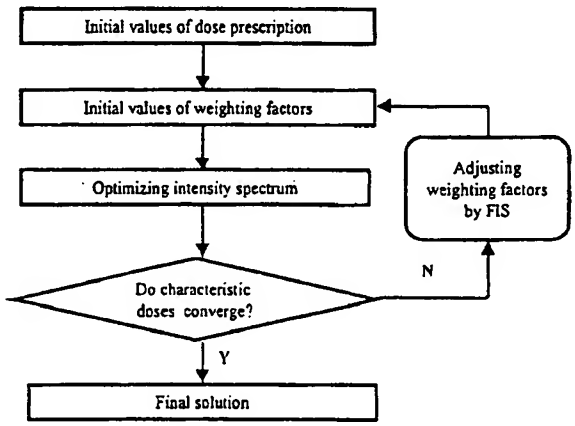
Initial values of dose prescription
Initial values of weighting factors
Optimizing intensity spectrum
Do characteristic doses converge?
N
Y
Adjusting weighting factors by FIS
Final solution

Fig. 4

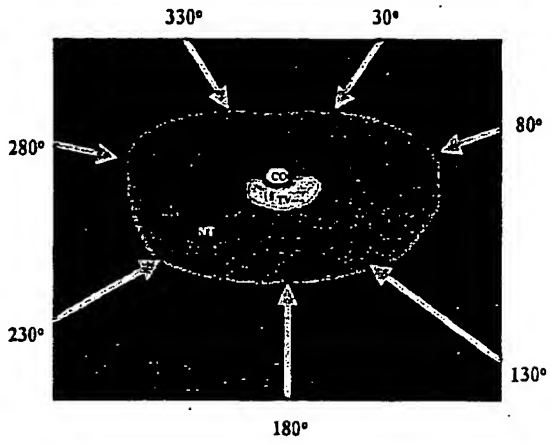
330°
30°
280°
80°
CC
NT
230°
130°
180°

Fig. 5a

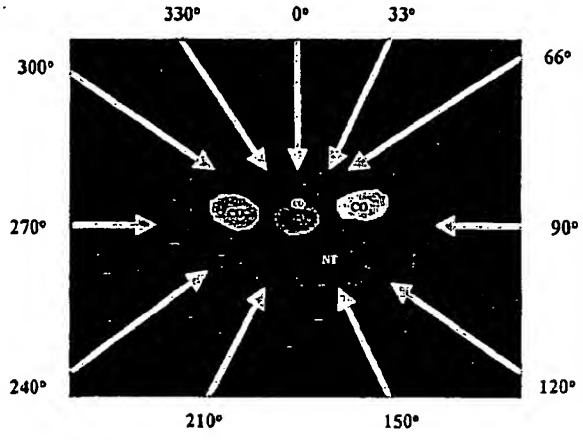
330°
0°
33°
300°
66°
270°
90°
NT
240°
120°
210°
150°

Fig. 5b

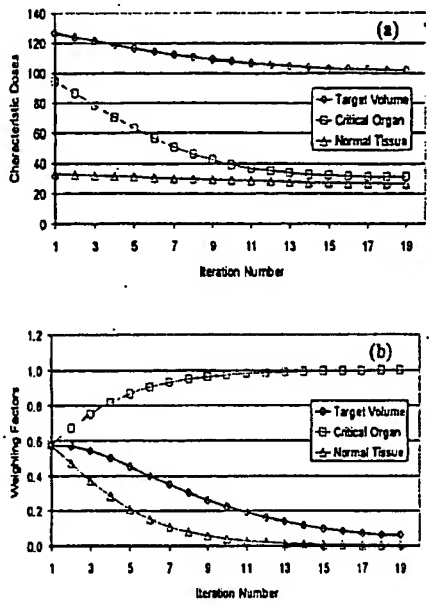
(a)
Characteristic Doses
Iteration Number
Target Volume
Critical Organ
Normal Tissue
(b)
Weighting Factors
Iteration Number
Target Volume
Critical Organ
Normal Tissue

Fig. 6

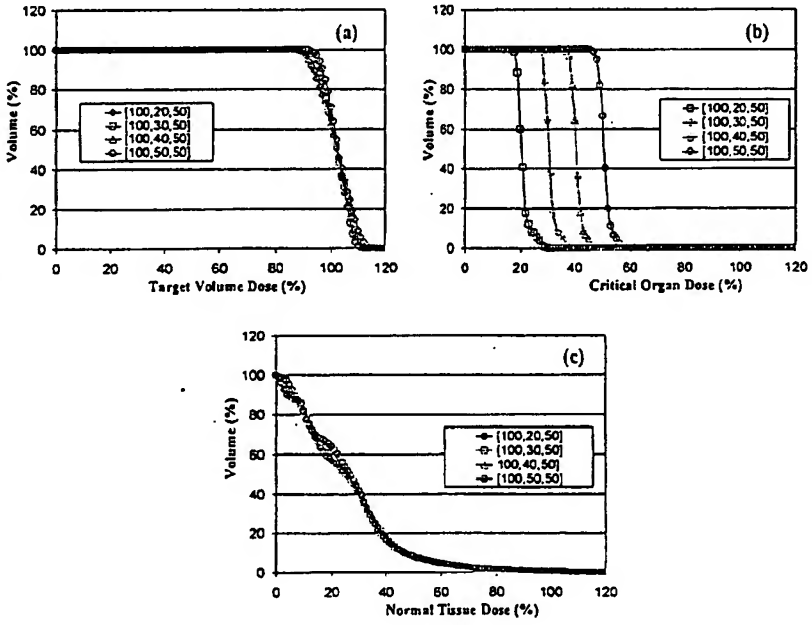
(a)
Volume (%)
Target Volume Dose (%)
[100,20,50]
[100,30,50]
[100,40,50]
[100,50,50]
(b)
Volume (%)
Critical Organ Dose (%)
[100,20,50]
[100,30,50]
[100,40,50]
[100,50,50]
(c)
Volume (%)
Normal Tissue Dose (%)
[100,20,50]
[100,30,50]
100,40,50]
[100,50,50]

Fig. 7

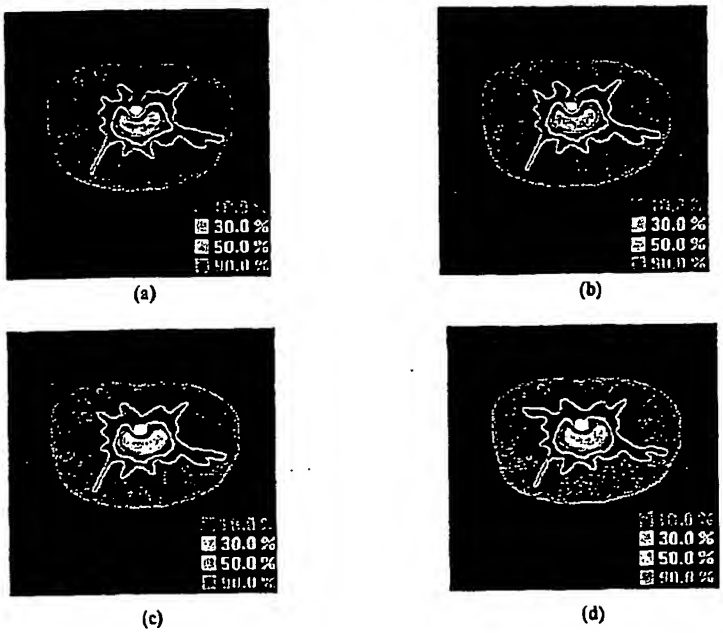
30.0 %
50.0 %
(a)
30.0 %
50.0 %
(b)
30.0 %
50.0 %
(c)
30.0 %
50.0 %
90.0 %
(d)

Fig. 8

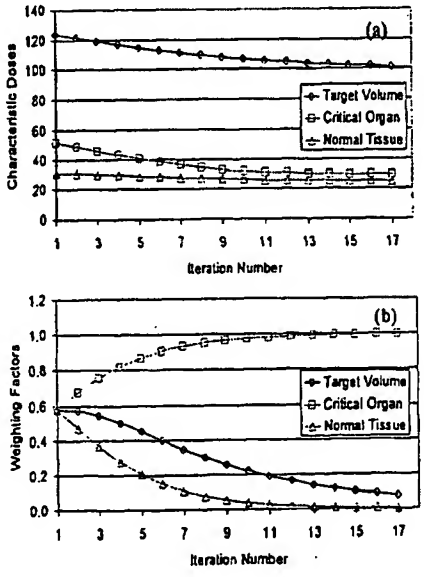
(a)
Characteristic Doses
Target Volume
Critical Organ
Normal Tissue
Iteration Number
(b)
Weighting Factors
Target Volume
Critical Organ
Normal Tissue
Iteration Number

Fig. 9

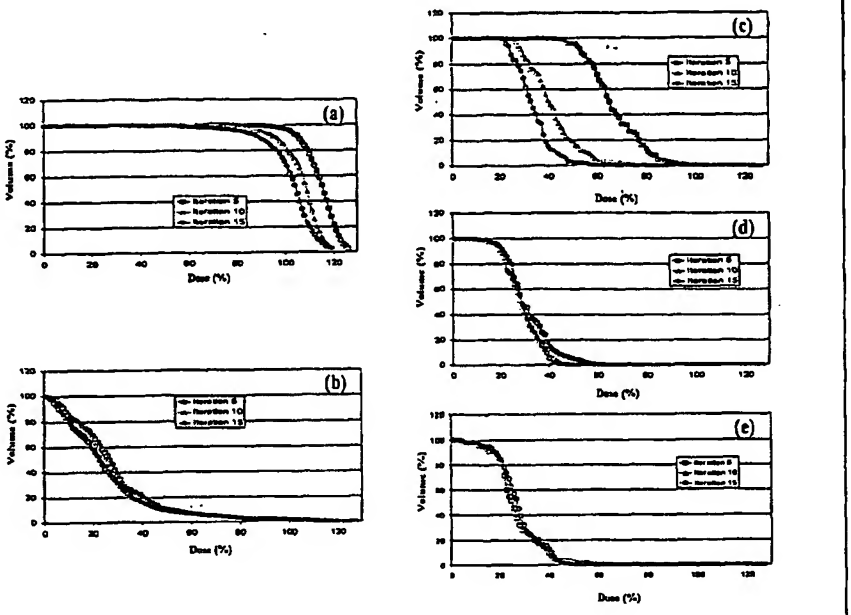

Fig. 10

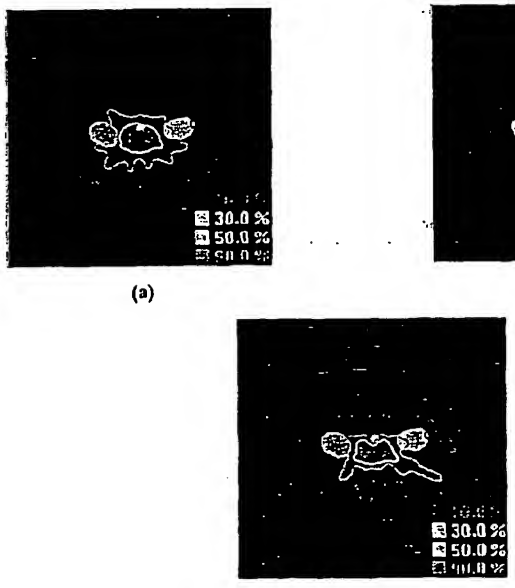

Fig. 11

Document made available under the Patent Cooperation Treaty (PCT)

International application number: PCT/US04/027893

International filing date: 27 August 2004 (27.08.2004)

Document type: Certified copy of priority document

Document details: Country/Office: US
Number: 60/498,742
Filing date: 28 August 2003 (28.08.2003)

Date of receipt at the International Bureau: 06 October 2004 (06.10.2004)

Remark: Priority document submitted or transmitted to the International Bureau in compliance with Rule 17.1(a) or (b)

World Intellectual Property Organization (WIPO) - Geneva, Switzerland
Organisation Mondiale de la Propriété Intellectuelle (OMPI) - Genève, Suisse

This Page is Inserted by IFW Indexing and Scanning Operations and is not part of the Official Record

BEST AVAILABLE IMAGES

Defective images within this document are accurate representations of the original documents submitted by the applicant.

Defects in the images include but are not limited to the items checked:

- ☐ BLACK BORDERS
- ☐ IMAGE CUT OFF AT TOP, BOTTOM OR SIDES
- ☐ FADED TEXT OR DRAWING
- ☐ BLURRED OR ILLEGIBLE TEXT OR DRAWING
- ☐ SKEWED/SLANTED IMAGES
- ☐ COLOR OR BLACK AND WHITE PHOTOGRAPHS
- ☐ GRAY SCALE DOCUMENTS
- ☑ LINES OR MARKS ON ORIGINAL DOCUMENT
- ☐ REFERENCE(S) OR EXHIBIT(S) SUBMITTED ARE POOR QUALITY
- ☐ OTHER: _____

IMAGES ARE BEST AVAILABLE COPY.

As rescanning these documents will not correct the image problems checked, please do not report these problems to the IFW Image Problem Mailbox.